



**UNIVERSIDAD DE INVESTIGACIÓN DE
TECNOLOGÍA EXPERIMENTAL YACHAY**

Escuela de Ciencias de la Tierra, Energía y Ambiente

**TÍTULO: Petrological study of the Cotacachi-Cuicocha
Volcanic Complex, Ecuador: Understanding the eruptive
dynamic and evolution of the magma**

Trabajo de integración curricular presentado como requisito para
la obtención del título de Geóloga.

Autor:

García Paredes Evelyn Raquel

Tutor:

Ph.D. Mandon Céline

Urcuquí, marzo del 2020

SECRETARÍA GENERAL
(Vicerrectorado Académico/Cancillería)
ESCUELA DE CIENCIAS DE LA TIERRA, ENERGÍA Y AMBIENTE
CARRERA DE GEOLOGÍA
ACTA DE DEFENSA No. UITEY-GEO-2020-00004-AD

En la ciudad de San Miguel de Urcuquí, Provincia de Imbabura, a los 6 días del mes de marzo de 2020, a las 13:00 horas, en el Aula CHA-01 de la Universidad de Investigación de Tecnología Experimental Yachay y ante el Tribunal Calificador, integrado por los docentes:

Presidente Tribunal de Defensa	Dr. VAZQUEZ TASET, YANIEL MISAEL , Ph.D.
Miembro No Tutor	Dr. SOLTANI DEHNAVI, AZAM , Ph.D.
Tutor	Dra. MANDON CELINE LUCIE , Ph.D.

Se presenta el(la) señor(ita) estudiante **GARCIA PAREDES, EVELYN RAQUEL**, con cédula de identidad No. **0104816566**, de la **ESCUELA DE CIENCIAS DE LA TIERRA, ENERGÍA Y AMBIENTE**, de la Carrera de **GEOLOGÍA**, aprobada por el Consejo de Educación Superior (CES), mediante Resolución **RPC-SE-10-No.031-2016**, con el objeto de rendir la sustentación de su trabajo de titulación denominado: **PETROLOGICAL STUDY OF THE COTACACHI-CUICOCHA VOLCANIC COMPLEX, ECUADOR: UNDERSTANDING THE ERUPTIVE DYNAMIC AND EVOLUTION OF THE MAGMA**, previa a la obtención del título de **GEÓLOGO/A**.

El citado trabajo de titulación, fue debidamente aprobado por el(los) docente(s):

Tutor	Dra. MANDON CELINE LUCIE , Ph.D.
--------------	----------------------------------

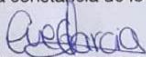
Y recibió las observaciones de los otros miembros del Tribunal Calificador, las mismas que han sido incorporadas por el(la) estudiante.

Previamente cumplidos los requisitos legales y reglamentarios, el trabajo de titulación fue sustentado por el(la) estudiante y examinado por los miembros del Tribunal Calificador. Escuchada la sustentación del trabajo de titulación, que integró la exposición de el(la) estudiante sobre el contenido de la misma y las preguntas formuladas por los miembros del Tribunal, se califica la sustentación del trabajo de titulación con las siguientes calificaciones:

Tipo	Docente	Calificación
Miembro Tribunal De Defensa	Dr. SOLTANI DEHNAVI, AZAM , Ph.D.	9,7
Tutor	Dra. MANDON CELINE LUCIE , Ph.D.	9,5
Presidente Tribunal De Defensa	Dr. VAZQUEZ TASET, YANIEL MISAEL , Ph.D.	9,6

Lo que da un promedio de: **9.6 (Nueve punto Seis)**, sobre 10 (diez), equivalente a: **APROBADO**

Para constancia de lo actuado, firman los miembros del Tribunal Calificador, el/la estudiante y el/la secretario ad-hoc.

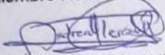

GARCIA PAREDES, EVELYN RAQUEL
Estudiante


Dr. VAZQUEZ TASET, YANIEL MISAEL , Ph.D.
Presidente Tribunal de Defensa


Dra. MANDON CELINE LUCIE , Ph.D.
Tutor

A. Soltani

Dr. SOLTANI DEHNAVI, AZAM , Ph.D.
Miembro No Tutor


TERÁN ROSALES, ANDREA YOLANDA
Secretario Ad-hoc

AUTORÍA

Yo, **Evelyn Raquel García Paredes**, con cédula de identidad 0104816566, declaro que las ideas, juicios, valoraciones, interpretaciones, consultas bibliográficas, definiciones y conceptualizaciones expuestas en el presente trabajo; así cómo, los procedimientos y herramientas utilizadas en la investigación, son de absoluta responsabilidad de el/la autor (a) del trabajo de integración curricular. Así mismo, me acojo a los reglamentos internos de la Universidad de Investigación de Tecnología Experimental Yachay.

Urcuquí, marzo del 2020.



Evelyn Raquel García Paredes

CI: 0104816566

AUTORIZACIÓN DE PUBLICACIÓN

Yo, **Evelyn Raquel García Paredes**, con cédula de identidad 0104816566, cedo a la Universidad de Tecnología Experimental Yachay, los derechos de publicación de la presente obra, sin que deba haber un reconocimiento económico por este concepto. Declaro además que el texto del presente trabajo de titulación no podrá ser cedido a ninguna empresa editorial para su publicación u otros fines, sin contar previamente con la autorización escrita de la Universidad.

Asimismo, autorizo a la Universidad que realice la digitalización y publicación de este trabajo de integración curricular en el repositorio virtual, de conformidad a lo dispuesto en el Art. 144 de la Ley Orgánica de Educación Superior.

Urcuquí, marzo del 2020.



Evelyn Raquel García Paredes

CI: 0104816566

DEDICATION

I dedicate this thesis to the love of my life, my son Atuk, because his eyes and hands were the main motivation to continue. Also, to my mom Raquel, because her support was crucial to keep studying. Moreover, her words of encouragement and her model inspired me to fight and succeed. I also dedicate this work to my dad, Jose Antonio; my sisters, Taty and Milagros; and my brother, Eddy. Thanks to them for the support, love, inspiration, and for believing in me. I would like to also dedicate this work to Fernando for accompanying me throughout the university and for his love. Finally, this thesis is specially dedicated to all of the student moms who were not able to continue their careers because of a lack of support. We keep on fighting for all of you.

With love,
Evelyn

ACKNOWLEDGMENTS

I want to express my sincere and special gratitude to my advisor Céline Mandon Ph.D., for her support, guidance, advice and patience; for sharing with me her knowledge and her love for volcanoes, for believing in me, and accepted to be my advisor. This thesis would never be done without her help and inspiration. Moreover, I want to thank my co-advisor Patricia Larrea, Ph.D., who, despite the distance, was always there for helping me; her comments were fundamental in this thesis. I would also like to acknowledge Elisa Piispa, Ph.D. for the donation of some thin sections, but also for joining us during field trips; her company and knowledge were always inspirational and made the field campaigns an enriching experience. Moreover, I acknowledge Azam Soltani, Ph.D., and Yaniel Vázquez, Ph.D., my committee members, for their valuable comments and suggestions on the written document and, especially, Azam for helping me with the estimation of mineral percentages.

I also want to thank Ministerio del Ambiente, Imbabura, for allowing us to sample rocks within the Cotacachi-Cayapas National Park. Especially to Veronica Pozo, in charge of the national park, to be always predisposed to help us and for allowing me to do an internship there. In this internship, I could know about the Cotacachi-Cuicocha Volcanic Complex and notice the potential and the importance of research on this. Furthermore, I would like to acknowledge Park Rangers of the Cotacachi-Cayapas National Park for their essential support during field trips, share their knowledge with us, and always be enthusiastic about learning geology. Also, I wish to thank Instituto de Investigacion Geologica y Energetico (IIGE), for allowing me to make thin sections. Mainly, Johanna León, liable of the Mineralogy and Petrographic Laboratory, and Ricardo Cabascango for his patience when teaching me how to prepare thin sections. Finally, I want to thank all my professors during my career for sharing their knowledge, inspiring me, and for their support and encouragement, especially Anna Foster Ph.D. and Alyssia Cox, Ph.D.

ABSTRACT

Ecuador is a country with 97 volcanoes, of which 13 are considered as active. Therefore, volcanic hazards are an important and concerning issue for Ecuadorians and their authorities. Most of these volcanoes are stratovolcanoes which usually present a complex and varied eruptive history. One of this, is the dormant Cotacachi volcano, which is part of the Cotacachi-Cuicocha Volcanic Complex (CCVC). This volcanic complex is located in the Western Cordillera of Ecuador and comprises, apart from the Cotacachi volcano, three satellite domes called Peribuela, Loma Negra and Muyurcu, and the Cuicocha caldera, which have four intra-caldera domes. The latest activity recorded of this volcanic complex was located on the southern flank of the Cotacachi volcano, with the growth of a fourth dome, destroyed in a caldera-forming eruption ~3.1 ka ago, and the growth of the four intra-caldera domes. In this thesis, data from a petrological study, which includes the use of an optical microscope and SEM coupled with an EDS detector, is presented, with an emphasis on the analysis of textures, chemical zonation, reaction rims in crystals and physical properties of the rocks from the CCVC. Textures such as oscillatory zoning, patchy zones, and sieve textures found in plagioclase crystals indicate kinetic effects and long-term processes within the magmatic chamber, decompression in magmas undersaturated in water, and magma mixing, respectively. Chemical zonation in pyroxene crystals shows different magma composition, and reaction rims in amphibole crystals reveal heating or decompression-induced processes that occurred during rim growth. Furthermore, the crystal population, their modal abundance, and vesicles were analyzed and related to viscosity. By considering all these data, we recognize some magmatic processes that occurred throughout the history of the CCVC, and we were able to reconstruct the magmatic history of the different eruptive phases of this volcanic complex.

Keywords: *domes, lava flows, textures, magmatic processes.*

RESUMEN

Ecuador es un país con 97 volcanes, de los cuales 13 se consideran activos. Por lo tanto, los peligros volcánicos son un tema importante y preocupante para los ecuatorianos y sus autoridades. La mayoría de estos volcanes son estratovolcanes que generalmente presentan una historia eruptiva compleja y variada. Uno de estos es el volcán inactivo Cotacachi, que forma parte del Complejo Volcánico Cotacachi-Cuicocha. Este complejo volcánico está localizado en la Cordillera Occidental del Ecuador y comprende, además del volcán Cotacachi, tres domos satélites llamados Peribuela, Loma Negra y Muyurcu, y la caldera Cuicocha, que tiene cuatro domos intra-caldera. La última actividad registrada de este complejo volcánico se localizó en el flanco sur del volcán Cotacachi, con el crecimiento de un cuarto domo, el cual fue parcialmente destruido durante una erupción que formó la caldera hace ~3.100 años, y el crecimiento de cuatro domos intra-caldera. En esta tesis, se presentan datos de un estudio petrográfico, que incluye el uso de un microscopio óptico y el SEM junto con un detector EDS, con énfasis en el análisis de texturas, zonación química, bordes de reacción en cristales y propiedades físicas de las rocas del Complejo Volcánico Cotacachi-Cuicocha. Texturas tales como zonación oscilatoria, zonación irregular y texturas de tamiz que se encuentran en los cristales de plagioclasa indican efectos cinéticos y procesos a largo plazo dentro de la cámara magmática, descompresión en magmas subsaturados en agua y mezcla de magma, respectivamente. La zonación química en los cristales de piroxeno muestra una composición de magma variada, y los bordes de reacción en los cristales de anfíboles revelan procesos de calentamiento o descompresión inducida que ocurrieron durante el crecimiento del borde. Además, la población de cristales, su abundancia modal y las vesículas fueron analizadas y relacionadas con la viscosidad. Al considerar todos estos datos, se reconocieron ciertos procesos magmáticos que ocurrieron a lo largo de la historia del Complejo Volcánico Cotacachi-Cuicocha, y así pudimos reconstruir la historia magmática de las diferentes fases eruptivas de este complejo volcánico.

Palabras clave: domos, flujos de lava, texturas, procesos magmáticos.

TABLE OF CONTENTS

AUTORÍA.....	v
AUTORIZACIÓN DE PUBLICACIÓN.....	vi
DEDICATION.....	vii
ACKNOWLEDGMENTS.....	viii
ABSTRACT.....	ix
RESUMEN.....	x
CHAPTER 1: INTRODUCTION	1
1.1 Problem Statement and Motivation	3
1.2 Objectives	4
CHAPTER 2: GEOLOGICAL FRAMEWORK.....	5
2.1 Cotacachi Volcano	7
2.2 Muyurcu Dome	7
2.3 Loma Negra Dome.....	8
2.4 Peribuela Dome.....	9
2.5 Pre-Cuicocha Caldera dome	10
2.6 Cuicocha caldera.....	10
2.7 Post-Cuicocha caldera domes	13
CHAPTER 3: METHODOLOGY	14
CHAPTER 4: RESULTS	17
4.1 Hand sample descriptions	17
4.2 Petrography	17
4.2.1 Cotacachi Volcano.....	18
4.2.2 Muyurcu dome.....	19
4.2.3 Loma Negra dome	20
4.2.4 Peribuela dome	20
4.2.5 Pre-Cuicocha caldera dome	20
4.2.6 Post-Cuicocha caldera domes.....	22

4.2.7	Enclave in Yerovi dome	23
4.3	SEM data.....	26
4.3.1	Amphibole rims	27
4.3.2	Plagioclase zoning and texture	30
4.3.3	Pyroxenes zoning.....	31
4.3.4	Enclave in Yerovi dome	32
CHAPTER 5: DISCUSSION		33
5.1	Amphibole rims	33
5.2	Plagioclase zoning and texture.....	35
5.3	Pyroxene zoning	36
5.4	Enclave in Yerovi dome	36
5.5	Viscosity, crystal content (size and modal abundance) and vesicles.....	36
5.6	Interpretation of the magmatic history of each volcanic center.....	37
CHAPTER 6: CONCLUSIONS		40
REFERENCES.....		41

CHAPTER 1: INTRODUCTION

Research in the field of volcanology is essential, mainly for two reasons, firstly to make efficient monitoring and early warning systems to safeguard people nearby volcanoes and secondly to increase our knowledge about the Earth's interior (Sigurdsson et al., 2015). There are many hazards associated with volcanoes such as lahars, ashfall, pyroclastic density currents (PDC), lava flows, volcanic gas, etc., which can cause damage to nearby infrastructure and even more, can put people's lives in danger. Therefore, understanding the evolution and behavior of volcanoes could be crucial to minimize the risk associated with volcanoes. Furthermore, studying and thus, understanding volcanoes will give us essential information about our planet and its evolution given that volcanoes are a manifestation of the cooling of our planet through heat and mass transfer from the core to the Earth's surface. Knowing the importance and benefit of the research on volcanoes, many areas have focused on studying the different processes related to their formation, evolution, dynamics, and eruptive style.

Igneous petrology is one of the most common areas, which studies the melts and rocks that crystallize from magmas, encompassing an understanding of the processes involved in melting, rise, crystallization, and eruption or emplacement of the rocks (Winter, 2014). In particular, petrological methods to study volcanic rocks focus on minerals, crystal textures and zoning, structures, and mineral populations, which are indicators of magmatic processes. For example, textural characteristics such as zoning patterns seen in some minerals can reflect changes in P, T, f_{O_2} and magma composition in a magmatic system (Viccaro et al., 2010). Different zones are formed under a specific magmatic environment and crystallization conditions. Thus, there are many magmatic processes such as convection, ascent-related depressurization, input of magma with different compositions, loss or input of volatiles, which are able to modify the physical and chemical parameters of a magmatic system and are also reflected in the way a crystal grows (Viccaro et al., 2010). Magma mixing, for example, can be reflected in chemical zonation, reaction rims and structural patterns in crystals (Słaby et al., 2008); a change in temperature, water content, pressure, oxygen fugacity of the system or composition also forms different growth textures (Renjith, 2014). Moreover, mechanical migration of crystals through areas with different T and/or composition causes zonal growth and textures in crystals (Słaby et al., 2008). In summary, the analysis of textures and crystal

zoning of rock-forming minerals can reveal the magmatic processes that occurred within the plumbing system and during emplacement.

Minerals such as plagioclase, amphibole, and pyroxene are crucial to understanding magmatic evolution of volcanic systems via their invaluable temporal archive of magmatic processes (Smith et al., 2009). For example, plagioclase group minerals crystallize over a wide temperature and compositional range of magma and can thus record physico-chemical fluctuations within a magma chamber in its compositional zoning (i.e., Costa Rodriguez et al., 2003; Pourkhorsandi et al., 2015). Additionally, plagioclase is highly sensitive to changes in temperature, pressure, melt composition and volatile content (Renjith, 2014; Viccaro et al., 2010), all of which are reflected in chemical variations in this mineral (Ginibre et al., 2007). Plagioclase also present a slow NaSi- CaAl diffusion (Stamatelopoulou-Seymour et al., 1990), and re-equilibrium rates (Salisbury et al., 2008), which allows preservation of a record of complex magmatic processes.

Reaction rims in minerals can also reveal complex magma ascent and mixing processes. For instance, reaction rims observed in amphibole are related to the release of structurally-bound water in response to decrease in water pressure in the melt as it ascends (Barker, 2014). The mineralogy and thickness of the reaction rim depends on processes that occurred during magma ascent, such as heating-induced and decompression-induced dehydration, direct contact with the host melt, and dehydrogenation and oxidation during magma extrusion (Angelis et al., 2015). For example, decompression-induced reaction rims are composed of orthopyroxene and plagioclase, with minor titanomagnetite, while heating reaction rims, which exist around anhedral and previously embayed crystal edges, are composed of clinopyroxene, calcic plagioclase, pargasite, and minor magnetite (Browne, 2005). In conclusion, the recognition of the minerals that compose the rims and the thickness of the reaction rims could tell us the process that occurred within the magma chamber and/or while magma ascent.

Moreover, recognition of plagioclase, amphibole and/or pyroxene populations based on shape, size, spatial distributions and internal features is an important step to describe the magma genesis and magmatic evolution of a volcanic system (Pallares et al., 2019). Cooling history of the magma can be inferred by crystal shape. For example, plagioclase morphology ranges from acicular to tabular and euhedral shapes, resulting from different degrees of cooling (Lofgren, 1974). Moreover, crystal size distribution can provide

information about nucleation and growth within the magma and spatial distribution constrain the nucleation distribution of crystals (Jerram and Martin, 2008). Therefore, the coexistence of different crystal populations provides key information on a variety of magmatic processes, such as magma mixing, magma mingling, crustal contamination, which can provide a better understanding of the magmatic systems.

Knowing how powerful is the analysis of minerals, textures, structures, crystal zoning and crystal populations to reveal magmatic processes, this thesis aims to make a petrological study to better understand the dynamics and evolution of the magmatic system throughout the history of the Cotacachi-Cuicocha Volcanic Complex (CCVC). Previous geological information about this volcanic complex is presented in chapter 2. The methodology used to fulfill the objectives of the present work is presented in chapter 3. In chapter 4, the data obtained are detailed, and in chapter 5, these data are discussed and analyzed. Finally, in chapter 6, the conclusions are presented together with the recommendations for future work.

1.1 Problem Statement and Motivation

Ecuador have no less than 97 volcanoes (Figure 2.1), out of which 13 are considered active. Among these, there is the Cuicocha volcano, which is part of the Cotacachi-Cuicocha Volcanic Complex (CCVC) that is located in the Imbabura province, northern Ecuador. Currently, the Cuicocha volcano shows diffuse gas emissions. It is therefore considered potentially active, representing a risk for the population living in Quiroga (6.400 pop) and Cotacachi (40.036 pop) regions located 10 km and 14 km away from the lake, respectively, as well as for the many tourists who visit the Cuicocha crater lake yearly.

Geologically speaking, the CCVC is of a special interest because it has had different effusive and explosive phases from localized emission of lava flows, dome-growing phase to Plinian eruption that led to the formation of the Cuicocha caldera. This shows very different eruptive styles throughout the history of this volcanic complex.

Moreover, few studies focused on CCVC (Almeida, 2016; Pidgen, 2014; Von Hillebrandt, 1989) and the Cuicocha crater lake (Bustos Gordón and Serrano, 2014; Cordero et al., 2019; Gunkel et al., 2011, 2009, 2008; Gunkel and Beulker, 2009; Melián et al., 2018).

In summary, the CCVC, a touristic attraction in the Imbabura province, is located in a populated area and has experienced varied eruptive activity within its lifetime. The motivation of this project is to increase our knowledge on this volcanic complex, especially on the potentially active Cuicocha volcano, of which very little is known up to date.

1.2 Objectives

Knowing how useful are petrological methods to reveal magmatic processes, therefore, understand volcanoes, the objectives of this thesis are:

- To make a petrological study using the SEM and optical microscope to describe textures, structures, crystal zoning and mineral populations of rocks from 3 satellite domes of Cotacachi volcano, the pre-Cuicocha caldera dome, the youngest post-caldera domes, and lava flows from Cotacachi volcano.
- To recognize some of the magmatic processes that occurred throughout the history of the CCVC and a better understanding of how magmas evolved and lead to a shift in volcanic activity.

CHAPTER 2: GEOLOGICAL FRAMEWORK

The volcanic activity in Ecuador is the result of the subduction of the Nazca Plate beneath the South American plate (Hall and Wood, 1985), which started between the Late Triassic and the Early Jurassic (Aspden et al., 1987; James, 1971; Pindell and Kennan, 2009). Quaternary volcanism is divided into three different domains: the volcanic front located on the Western Cordillera (WC), the main arc located in the Interandean Valley and the Eastern Cordillera, and the back arc which is built over the headwaters of the Amazon basin (Hall et al., 2008) (Figure 2.1). According to Hormann and Pichler (1982), magmas from the volcanoes of the Western Cordillera, where the CCVC is located, belong to the andesite-plagioclase series, which is characterized by 1 ± 0.2 wt% K_2O content, low abundances of large ion lithophile elements LILE (Rb, Sr and-Ba), high field strength elements HFSE (Zr, U and-Th) and relatively high Ni and Cr abundances. Moreover, Cenozoic magmas of the WC are suggested to be formed by partial melting of a basaltic amphibolite of olivine tholeiitic composition in the subduction zone beneath the Andean Cordillera at a depth of about 70 km (Hormann and Pichler, 1982). Hall et al. (2008) also established that the Late Pleistocene and Holocene activity of the volcanic centers located in the WC were andesitic to dacitic in composition and the rocks have SiO_2 content that ranges from 60 to 66% and K_2O content ranging from 0.9 to 1.5%. Moreover, the lavas of the WC show adakitic characteristics. In addition, the lowest $^{87}Sr/^{86}Sr$ and the highest $^{143}Nd/^{144}Nd$ ratios demonstrate a younger, more mafic crust is under the WC compared to the more sialic crust beneath the Eastern Cordillera (Hall et al., 2008).

The Cotacachi-Cuicocha Volcanic Complex (CCVC) is located in the Northern part of the Western Cordillera of Ecuador (Figure 2.1), along the Otavalo-Umpalá fracture zones. This volcanic complex comprises the Cotacachi volcano, three satellite domes called Loma Negra, Peribuela and Muyurcu, a remnant of the pre-Cuicocha caldera dome, the Cuicocha caldera, nowadays a lake, and four intra caldera domes that forms two islands called Teodoro Wolf and Yerovi inside the lake (Figure 2.2). Geological information focusing on the different units of the CCVC collected from previous research (Almeida, 2016; Bablon, 2019; Pidgen, 2014; Von Hillebrandt, 1989) is presented below.

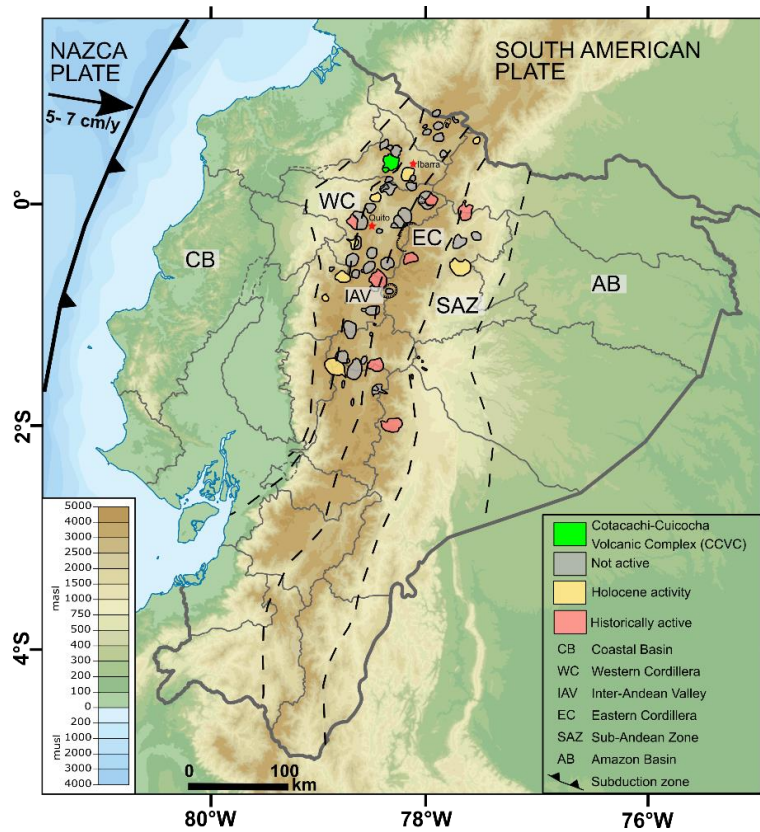


Figure 2.1 Ecuadorian volcanoes distribution map, showing the location of the Cotacachi-Cuicocha Volcanic Complex (CCVC). Also represented are the Coastal Basin, the Western Cordillera, the Inter-Andean Valley, the Eastern Cordillera, the Sub-Andean Zone and the Amazon Basin, from East to West. Different blue, green and brownish colors represent elevation in meters under sea level (mssl) and above sea level(masl) respectively.

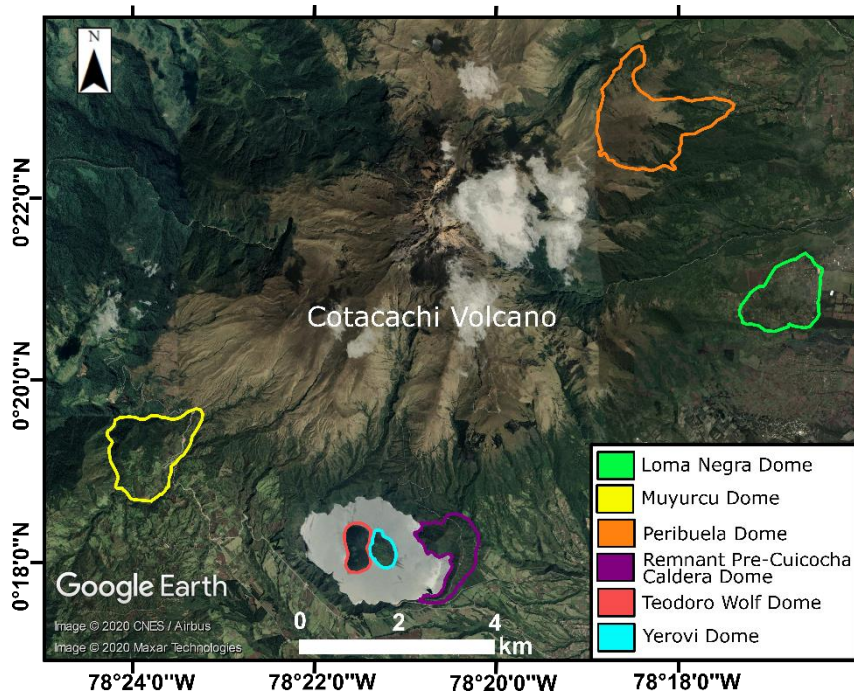


Figure 2.2 Satellite Google Earth image of the Cotacachi-Cuicocha Volcanic Complex showing the units of interest in this study. Based on Almeida (2016) and Von Hillebrandt (1989).

2.1 Cotacachi Volcano

Cotacachi volcano (4939 masl, Figure 2.2 and 2.3), the central edifice of the CCVC, has a ~ 12 km diameter at the base. Its volcanic activity started in the Pleistocene (~180 ka) (Bablon, 2019), and it is composed of massive intercalations of lava flows and volcanic breccia deposits (Almeida, 2016). Some of the lava flows reached as far as 18 km away from the central emission point and are pyroxene-andesite in composition (Von Hillebrandt, 1989).



Figure 2.3 North-eastern view of the Cotacachi volcano from Urcuqui town. The highest peak and the summit lavas are observed. Credits: C Mandon in 2019.

2.2 Muyurcu Dome

Muyurcu dome (3502 masl, Figures 2.2 and 2.4) is located in the southwestern flank of the Cotacachi volcano and is composed of grey vesiculated and porphyritic andesites. This dome comprises three little domes occupying an area of ~2 km², that were preceded by lava flow emplacement (Almeida, 2016; Pidgen, 2014; Von Hillebrandt, 1989). According to Bablon (2019), this dome has an age of 138 ± 4 ka.



Figure 2.4 North-eastern view of Muyurcu dome. Credits: C Mandon in 2019.

2.3 Loma Negra Dome

Loma Negra (3055 masl, Figure 2.2 and 2.5) is located in the southeast flank of the Cotacachi volcano. It had three different activity phases, which include dome formation and collapse producing various PDCs and associated ash falls (Von Hillebrandt, 1989). According to Almeida (2016) and Von Hillebrandt (1989), this dome is more than 40 ka, and presents amphibole, plagioclase and few pyroxene, being classified as hornblende-rich andesites (i.e. >40%).



Figure 2.5 Northern view of Loma Negra dome. Credits: C Mandon in 2019.

2.4 Peribuela Dome

Peribuela dome (3864 masl, Figure 2.2 and 2.6) occupies part of the northeastern flank of Cotacachi volcano and is the biggest of the domes with an area of 4.5 km². According to Von Hillebrandt (1989), it is composed of hornblende-rich dacites, while Almeida (2016) argues an andesitic composition. This dome, which is younger than Loma Negra but older than the pre-Cuicocha caldera dome (Von Hillebrandt, 1989), had two activity phases with PDCs and ash falls (Pidgen, 2014; Von Hillebrandt, 1989).



Figure 2.6 Eastern view of Peribuela Dome and the scar left from a sector collapse. Credits: C Mandon in 2019.

2.5 Pre-Cuicocha Caldera dome

A remnant of the pre-Cuicocha caldera dome (3377 masl, Figure 2.2 and 2.7) is located in the southwestern flank of the Cotacachi volcano and is part of the eastern edge of the Cuicocha caldera. This remnant is composed by an amphibole-rich andesite (Almeida, 2016) to dacite (Pidgen, 2014) rock. The pre-Cuicocha caldera dome used to be ~1.5 km diameter (Von Hillebrandt, 1989).

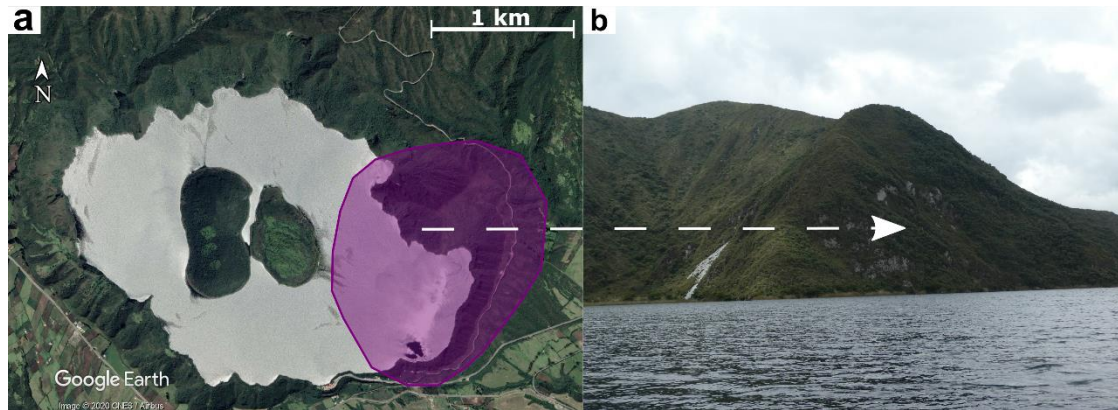


Figure 2.7 a) Model extent of the pre-Cuicocha caldera dome prior to the formation of the Cuicocha caldera according to (Von Hillebrandt, 1989); b) South-western view of the remnant of the Pre-Cuicocha caldera dome. Credits: C Mandon in 2019.

2.6 Cuicocha caldera

The Cuicocha caldera (3072 masl and Figure 2.7) has a diameter of 3.2 km, a maximum depth of 450 m and nowadays is filled by a lake (148 m deep, 0.28 km³ in volume) formed by the deglaciation of the Cotacachi volcano, rainwater and hydrothermal water (Padrón et al., 2008). The caldera was formed by an eruption of the Cuicocha satellite dome, which existed prior to the caldera formation (Pidgen, 2014).

Pidgen (2014) proposed four different stages of activity of the Cuicocha volcano (Figure 2.8). The first stage corresponds to a Plinian eruption which destroyed the Cuicocha dome. This climactic eruption occurred 3.1 ka and resulted in 4.1 km³ of flow-dominated PDCs and the caldera collapse. Then the activity switched to the formation of a new dome, with water accumulation in the caldera. An explosive phase started again after ~110 years. The newly-formed dome was destroyed and smaller volume of juvenile material was ejected. This stage is characterized by surge-dominated PDCs during phreatomagmatic eruptions. Finally, the activity resumed with the growth of four intra caldera domes which

nowadays are two islands (Teodoro Wolf and Yerovi) in the center of the Cuicocha crater lake (Pidgen, 2014; Von Hillebrandt, 1989).

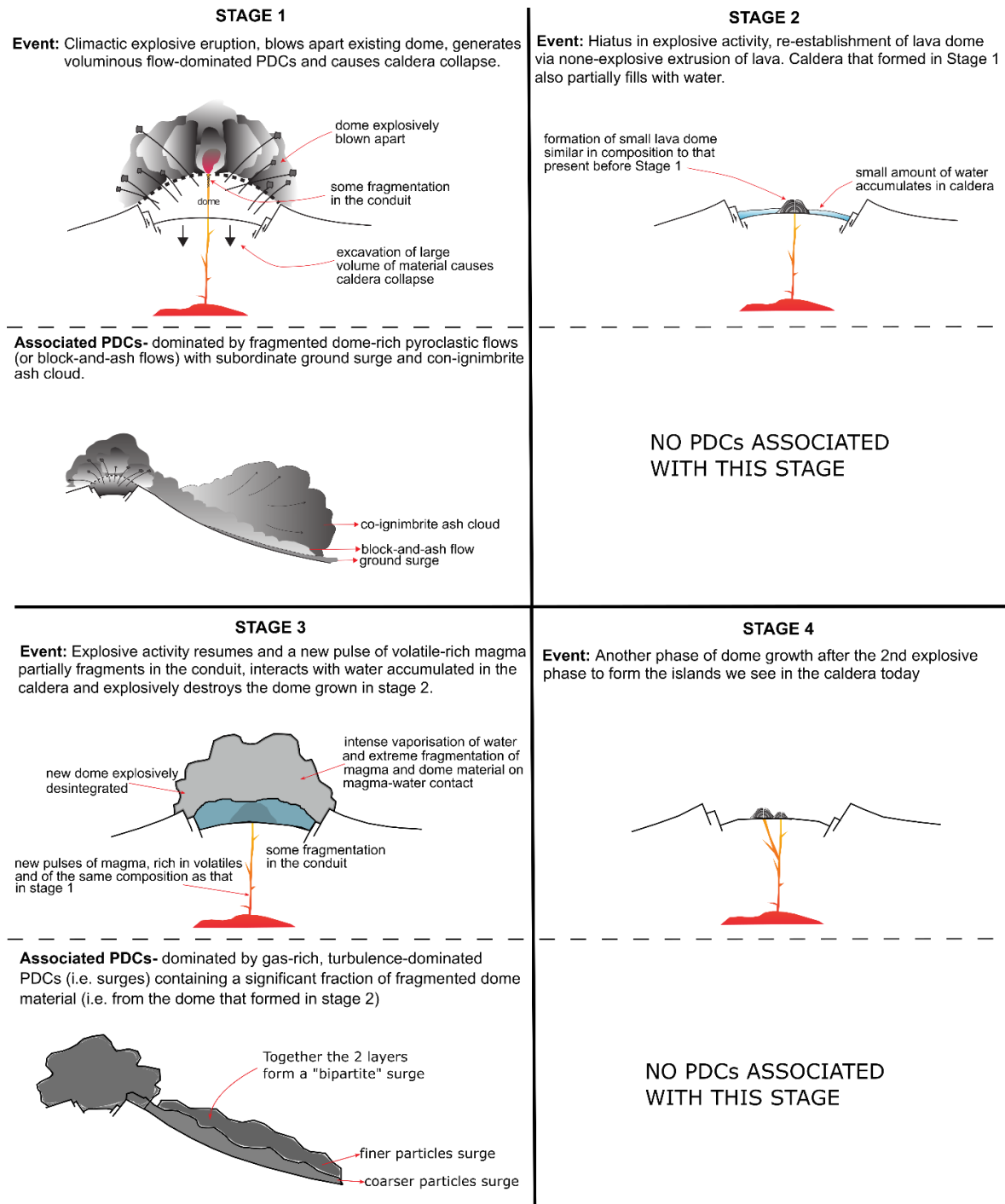


Figure 2.8 A conceptual synthesis of the series of events at Cuicocha volcano. In stage 1, the Cuicocha volcano activated by an eruption which destroyed the dome and formed a caldera. In stage 2, there was a hiatus where water accumulate within the caldera while a dome was growing. In stage 3, explosive activity resumed destroying the newly formed dome. Finally, in stage 4, a phase of dome-growth occurred forming Teodoro Wolf and Yerovi islands (Pidgen, 2014).

Nowadays, the Cuicocha caldera is considered an active volcano. It presents post-volcanic activities such as diffuse emission of volcanic gases and input of hydrothermal waters at the bottom of the lake (Gunkel and Beulker, 2009; Padrón et al., 2008). The continuous emission of gases which rise through fractures beneath the lake bottom as bubbles indicates degassing of the remaining magma body (Gunkel et al., 2009). According to Bustos Gordón (2014), in 2006 the amount of CO₂ released to the atmosphere was 106 t.d⁻¹ (metric tons per day), in 2012, 652 t.d⁻¹, and in 2014 was 95 t.d⁻¹. The latest survey campaigns in September 2017 and October 2018 revealed 244 tons and 76 tons of CO₂ emitted daily respectively (Cordero et al., 2019; Melián et al., 2018). Moreover, an increase in the seismic activity of this volcano was recorded in October 2018, with 62 earthquakes (volcano tectonic type) up to a magnitude of 2.5 (Córdova et al., 2018). For these reasons the Cuicocha crater lake is considered an active volcano and therefore has a monitoring network, installed by the Instituto Geofísico of Ecuador, the institution in charge of monitoring the Ecuadorian volcanoes, which consists on seismometers, GPS and a CO₂ meter distributed around the caldera lake (Figure 2.9).

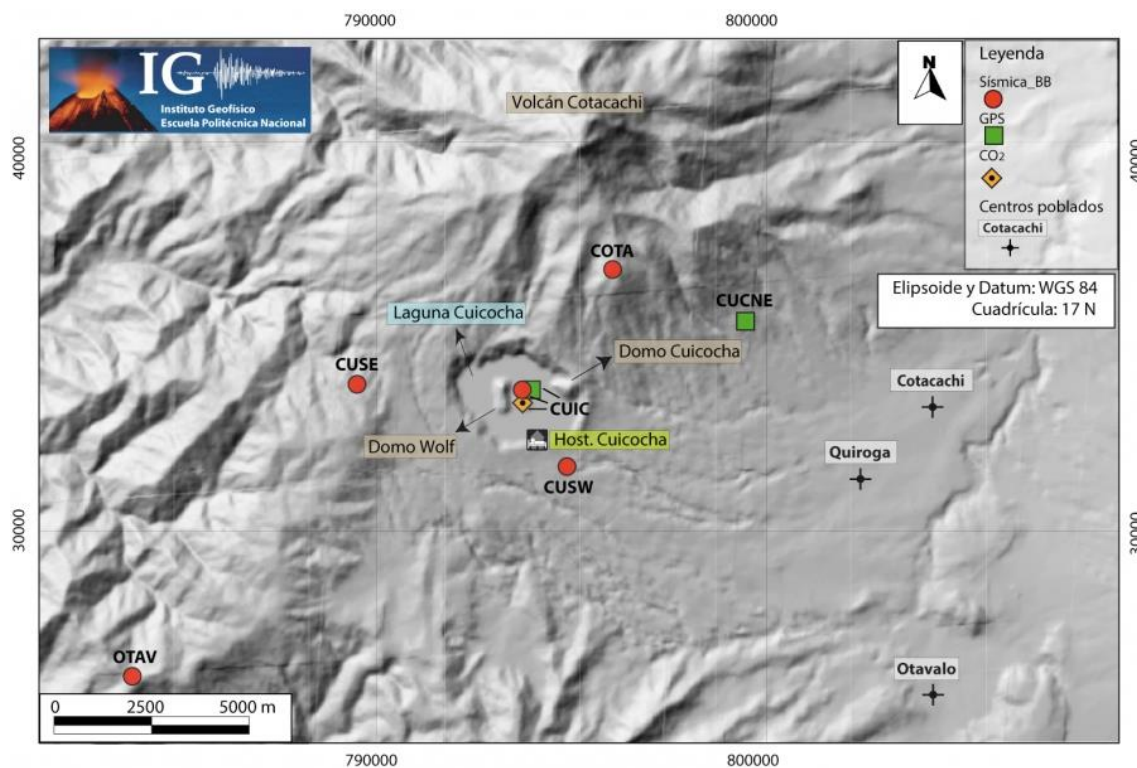


Figure 2.9. Monitoring network of the Cuicocha caldera installed and controlled by the Instituto Geofísico-EPN (IG-EPN). Taken from IG-EPN web page.

2.7 *Post-Cuicocha caldera domes*

Yerovi (3062 masl, 0.26 km²) and **Teodoro Wolf** (3247 and 3202 masl for the North and South domes respectively, 0.44 km²) islands are located in the center of the Cuicocha crater lake (Figure 2.10) and are formed by four post-caldera domes which are the last evidence of the Cuicocha volcano activity (Gunkel et al., 2009). According to Almeida (2016) and Pidgen (2014) the post-caldera domes are composed of dacite.



Figure 2.10 North-eastern view of the Cuicocha lake that fills the caldera, and the four post- caldera domes. Credits: C Mandon in 2018.

Table 3.1 Coordinates of the sampled rocks in the CCVC during January-June 2019.

Location	Sample Name	Coordinates in degrees minutes seconds
Muyurcu dome	CI1	0°19'29" N, 78°23'58" W
Loma Negra dome	CI2	0°21'1" N, 78°17'11" W
Yerovi dome	CI3	0°18'15" N, 78°21'36" W
Cotacachi lava flow: northern shore of Cuicocha	CI4	0°18'35" N, 78°21'26" W
Pre-Cuicocha caldera dome	CI5	0°18'23" N, 78°21'12" W
Cotacachi lava flow: Las Antenas	CI6	0°19'53" N, 78°20'34" W
Teodoro Wolf Southern dome	CI7	0°18'6" N, 78°22'1" W
Teodoro Wolf Northern dome	CI9	0°18'20" N, 78°21'48" W
Peribuela dome	CI10	0°23'6" N, 78°18'46" W

All of the sampled rocks were described in hand sample, then, representative thin sections were made at the *Instituto de Investigación Geológica y Energética* (IIGE) in Quito-Ecuador. An optical microscope at Yachay Tech was used to identify minerals, describe the rock structures, and characterize mineral populations and modal abundances for each thin section.

Mineral modes were estimated using the “Background” tool of *JMicroVision v1.3.1* software. For this, the thin sections were scanned with a high-quality printer and uploaded to the program for analysis. The “Background Extraction” was made with specific threshold depending on the mineral of interest. This tool was used to calculate the percentage of matrix and the different minerals without taking into account their size. Modal abundance of microphenocrysts (>100 µm and <700 µm) and phenocrysts (>700 µm) for each mineral were obtained with the optical microscope together with a visual chart for determining the approximate modal (volume) percentage of minerals in rocks. Moreover, all mineral abbreviations used in the present study are in accordance to Whitney and Evans (2010), except for pyroxene crystals, for which Pxs will be used.

Furthermore, a JEOL IT 300 SEM coupled with EDS detector at the *Instituto Nacional de Patrimonio Cultural* in Quito was used for imaging and semi-quantitative analysis. SEM is an imaging instrument which can give us secondary electron (SE) images, that shows topographic features and backscattered electron (BSE) images which reveal compositional variations (Reed, 2005). BSE images originate from elastic collisions between the incident electron beam and atomic nuclei at the sample surface (Blundy and

Cashman, 2008). This type of images can show zoning patterns given that the compositional variations related to changes in the mean atomic weight are seen in the brightness of the image (Streck, 2008). Regions with high atomic number will appear bright relative to regions where the atomic number is low (Goldstein, Joseph Newbury et al., 2003). Therefore, it is possible to easily identify different zoning patterns in crystals, related to differences in composition, so we can obtain information about the processes that occurred during the crystallization of certain mineral, consequently, the behavior of the magmatic system.

In the present study, BSE images of rimmed amphibole in rock samples from Loma Negra dome, Yerovi dome, pre-Cuicocha caldera dome and Cotacachi lava flow were taken, as well as zoned plagioclase in rock samples from Loma Negra and pre-Cuicocha caldera dome, and pyroxene in rocks from Muyurcu dome and Cotacachi lava flow. High-resolution images of the contact between the enclave in Yerovi sample and the host rock were taken too. In addition, EDS point analyses were performed for those amphiboles with reaction rims from Loma Negra, Yerovi and the Cotacachi lava flow. For the amphibole of the Cotacachi lava flow, four-point analyses were made, three in different parts of its rim and one in the core. For Loma Negra and Yerovi the analyses were performed just in one point of the core and rim. The point analyses were made using an acceleration voltage of 20 kV.

CHAPTER 4: RESULTS

4.1 *Hand sample descriptions*

All the rock samples present a porphyritic texture. The main difference between the samples is the amount and the size of crystals. Sample C14 from the Cotacachi lava flow and Muyurcu dome (CI1) contain Pxs and Pl phenocrysts. In Cotacachi lava flow (CI4), Pxs and Pl are anhedral and the smallest compared to all the rock samples (<1 mm). In Muyurcu dome, Pxs and Pl are bigger and euhedral; plagioclase phenocrysts are maximum 4 mm in size, while Pxs phenocrysts are maximum 2 mm. The other Cotacachi lava flow sampled in “Las Antenas” (CI6), includes euhedral Amp phenocrysts, showing maximum size of 5 mm. The amount of Pxs phenocrysts is lower than Amp phenocrysts. Loma Negra dome sample (CI2) contains some Amp phenocrysts that are euhedral and ~1 to 3 mm in size, as well as Pl phenocrysts that are subhedral to anhedral, having size range from 0.5 to 4 mm. In post-Cuicocha caldera domes (CI3 and CI7) the Amp phenocrysts (1 to 6 mm in size) are euhedral, occurring in higher abundance compared to all the studied samples. Pl phenocrysts in CI3, CI7 and CI9 samples are euhedral and the biggest (2 to 6 mm) compared to the other rock samples. Finally, pre-Cuicocha caldera (CI5) and Peribuela (CI10) domes present euhedral Amp phenocrysts with a size of 1 to 6 mm and Pl phenocrysts from 1 to 3 mm. In terms of color, rocks from the Cotacachi lava flows are grey; from Muyurcu and the post-Cuicocha caldera domes are light grey; from Loma Negra presents a light pinkish color and from pre-Cuicocha caldera and Peribuela dome are white-ish.

An enclave, found in sample CI3 from Yerovi dome, presents a plutonic texture and a darker color than the host rock. This enclave is 2 x 1.5 cm in size and consists in anhedral Amp (<1 mm in size) and Pl (less than 1 mm to 2 mm in size). Very few euhedral Amp (~2 mm in size) are also identify.

4.2 *Petrography*

Mineral modes, textures, presence or not of zonation and reaction rims of minerals from the different units of the CCVC are presented below. Moreover, to better visualize and analyze all these data, Table 4.1 summarizes the information.

4.2.1 *Cotacachi Volcano*

The sample CI6 displays a trachytic texture and is composed of ~6% of phenocrysts, 49% of microphenocrysts (>100 and < 700 μm) and 45% of groundmass. The phenocrysts are 2% Pl, 3% Amp and <1% of Pxs. The microphenocrysts are composed by 2% Amp, 35% Pl, 10% Pxs and 2% opaque minerals. The two populations of Amp (microphenocrysts and phenocrysts) are elongated acicular (Figure 4.1a) or hexagonal in shape, showing thick dark reaction rims of ~55 μm thickness. Also, some Amp demonstrate skeletal texture. Amp are surrounded by fine-grained anhedral Pxs (bright yellow points) which are delineated by dashed white lines in Figure 4.1b. Some of the Pl phenocrysts display oscillatory zoning. Pyroxene phenocrysts and microphenocrysts are commonly forming glomerocrysts (Figure 4.1c). The groundmass is composed by Pl and Pxs microlites (<100 μm).

Trachytic texture is also seen in sample CI4. This sample is composed of 8% of phenocrysts, 57% of microphenocrysts and 35% of groundmass. The phenocrysts are 3% Pl and 5% Px, the microphenocrysts are 40% Pl, 15% Px and 2% opaque minerals. The plagioclase phenocrysts display oscillatory zoning with wavy zoning surfaces and fine-sieved zoning (Figure 4.1d). Individual Px phenocrysts as well as glomerocrysts of Px are observed (Figure 4.1e and 4.1f).

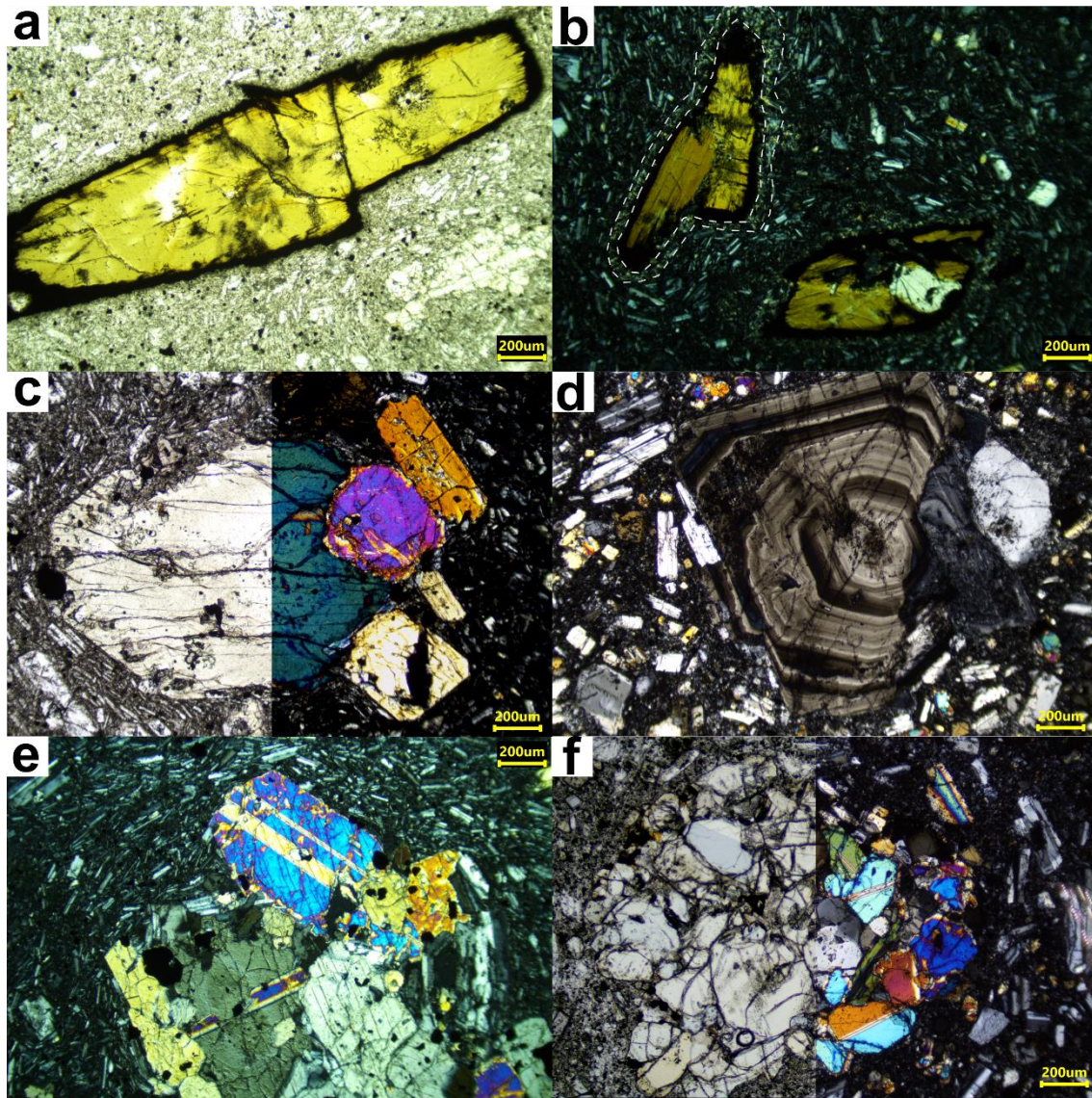


Figure 4.1 Representative photomicrographs of crystals from the Cotacachi lava flow taken with an optical microscope. a) Amphibole phenocryst with thick dark rim, sample CI6 (PPL); b) Amphibole microphenocrysts with thick dark rim surrounded by fine-grained Pxs (delineated by dashed white lines) and trachyte texture, sample CI4 (XPL); c) Glomerocrysts of microphenocrysts of Px, sample CI6 (right: XPL; left: PPL); d) Oscillatory zoned phenocrysts of Pl, with wavy and fine-sieved areas, sample CI4 (XPL); e) Glomerocrysts of microphenocrysts of Pxs with trachyte texture around the cluster, sample CI4 (XPL); f) Glomerocrysts of microphenocrysts of Pxs, sample CI4 (right: XPL; left: PPL).

4.2.2 *Muyurcu dome*

CI1 presents a porphyritic texture and contains 20% phenocrysts, 55% microphenocrysts, 15% groundmass, and 10% of vesicles. The phenocrysts are composed of 10% Pl and 10% Pxs. The microphenocrysts are composed by 30% Pl, 20% of Pxs and 5% opaque minerals. Plagioclase crystals are euhedral and some of them showing zoning, Pxs morphology varies from subhedral to euhedral and there are glomerocrysts of just Pxs and Pxs with Pl (Figure 4.2a).

4.2.3 *Loma Negra dome*

CI2 presents a porphyritic texture, consisting 12% of phenocrysts, 58% of microphenocrysts, 20% of groundmass and 10% of vesicles. The phenocrysts are 10% Pl glomerocrysts and 2% elongated acicular or hexagonal Amp. The last mineral present skeletal texture and dark thin reaction rims (~18 μm). Some Amp phenocrysts present remnant of a reaction rim composed of Pl and Pxs (Figure 4.2b). In terms of microphenocrysts, 35% are zoned Pl, 5% glomerocrysts of Px, 8% Amp and 10% Opq. Few Pl present sub-rounded and embayed spongy cores and oscillatory zoning (Figure 4.2c and 4.2d). The groundmass is composed of Pl microlites.

4.2.4 *Peribuela dome*

CI10 presents a porphyritic texture, having 27% of phenocrysts, 40% of microphenocrysts and 33% of groundmass. Phenocrysts are composed of 20% Pl, 5% Amp and 2% Bt. The microphenocrysts are 25% Pl, 5% Amp, 8% biotite and 2% Opq. The groundmass contains Pl microlites. The two Amp populations are hexagonal or elongated acicular with some presenting a skeletal texture, also they present thin dark rims (~12 μm) (Figure 4.2e). The two populations of Pl present sieve zoning and oscillatory zoning with wavy zoning surfaces (Figure 4.2f). Plagioclase and Amp sometimes occur as glomerocrysts.

4.2.5 *Pre-Cuicocha caldera dome*

CI5 presents a porphyritic texture and is composed of 40% phenocrysts, 25% microphenocrysts, 25% groundmass and 10% vesicles. The phenocrysts are 35% zoned Pl as isolated crystals and in glomerocrysts, and 5% Amp. The microphenocrysts are 15% Amp, 5% Pl and 5% Opq. The Amp are elongated acicular or hexagonal, presenting a skeletal texture and black rims of ~15 μm (Figure 4.2g). The Pl shows oscillatory zoning, patchy zoning with glass inclusions, and sub-rounded cores surrounded by oscillatory outer layer (Figure 4.2h). The groundmass is composed of Pl microlites.

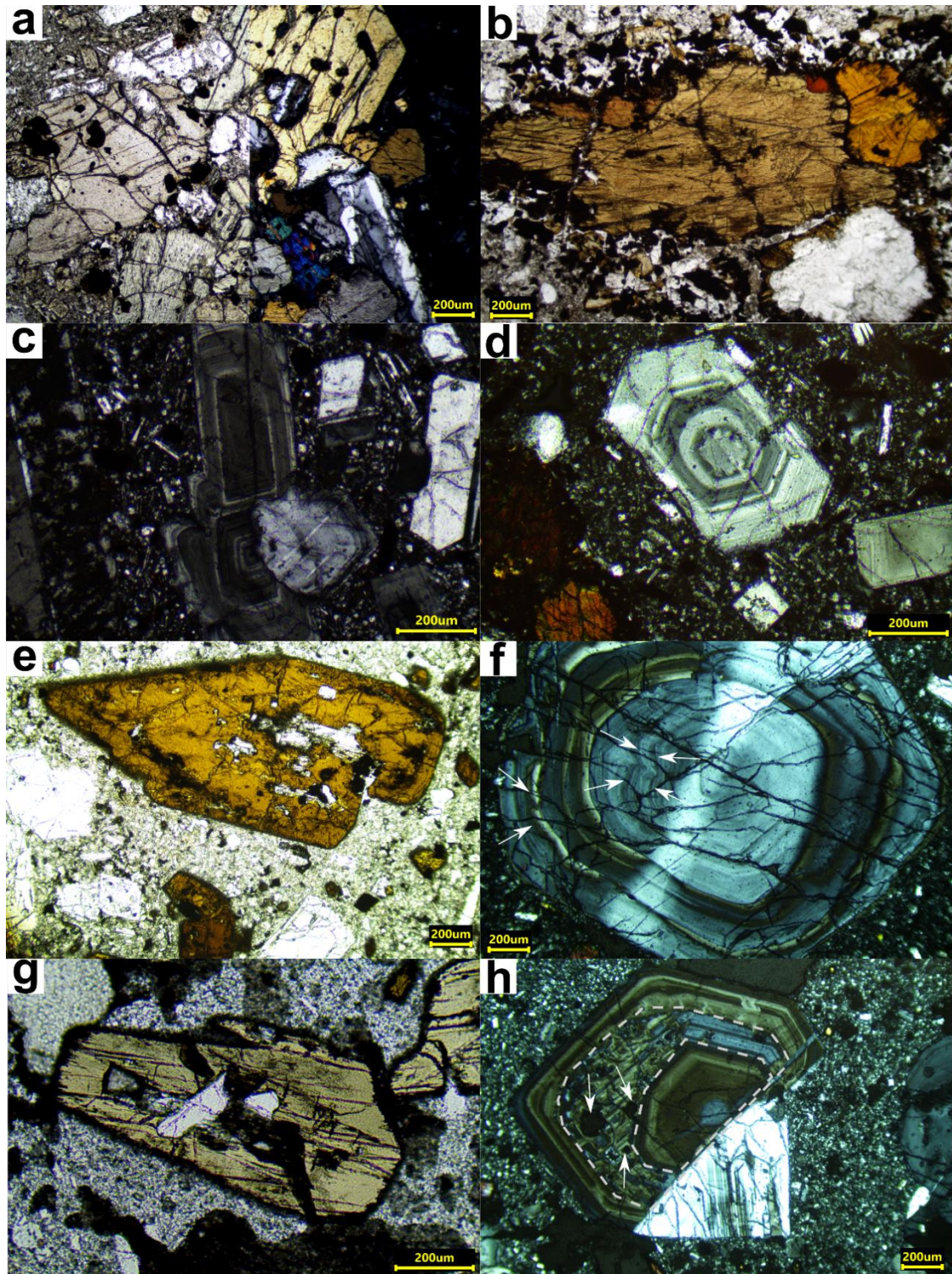


Figure 4.2 Representative photomicrographs of crystals from the satellite domes of the CCVC taken with an optical microscope. a) Glomerocrysts of Px with Pl, sample Muyurcu dome (CI1) (XPL); b) Amphibole phenocrysts with thick breakdown rim, sample Loma Negra (CI2) (PPL); c) Zoned Pl phenocryst, sample Loma Negra (CI2) (XPL); d) Rounded core surrounded by oscillatory zoning microphenocryst of Pl, sample Loma Negra (CI2) (XPL); e) Skeletal Amp, sample Peribuela dome (CI10) (PPL); f) Zoned Pl phenocryst with wavy zoning surfaces (indicated by white arrows), sample Peribuela dome (CI10) (XPL); g) Microphenocryst of rimmed Amp with skeletal texture, sample pre-Cuicocha caldera (CI5) (PPL); h) Patchy texture (delineated by white dashed lines) with glass inclusions (indicated by white arrows) and oscillatory zoned Pl, sample pre-Cuicocha caldera (CI5)(XPL).

4.2.6 *Post-Cuicocha caldera domes*

Yerovi dome (CI3) presents a porphyritic texture and is composed of 45% of phenocrysts, 20% of microphenocrysts, 25% microlitic groundmass of plagioclase and 10% vesicles. The phenocrysts are 40% of glomerocrystals of plagioclase and 5% of amphiboles. The microphenocrysts are 10% Amp, 5% Pl and 5% opaque minerals. The Amp present a thin rim (~10 μm), are hexagonal or rectangular elongated and, especially the phenocrysts, have a skeletal texture (Figure 4.3a, 4.3b). Plagioclase presents oscillatory zoning (Figure 4.3c), occasionally showing wavy zoning surfaces.

Teodoro Wolf dome (CI7 and CI9) with a porphyritic texture is composed of 50% of phenocrysts, 23% of microphenocrysts, 24% of groundmass with Pl microlites and 3% of vesicles. The phenocrysts are 45% zoned Pl glomerocrysts (>1 mm) and 5% Amp as individual crystals or as glomerocrysts. The microphenocrysts are 15% Amp, 5% Pl and 3% of opaque minerals. The Amp are elongated acicular or hexagonal shaped with very thin rim (~12 μm thickness) and few present a skeletal texture (Figure 4.3d). As in Yerovi dome, the Amp phenocrysts are the ones that specially present a skeletal texture. There are also glomerocrysts of Pl with Amp. Plagioclase displays a wide variety of textures such as oscillatory zoning with sub-rounded cores (Figure 4.3e) and patchy cores with glass inclusions surrounded by wavy zoning surfaces (Figure 4.3f).

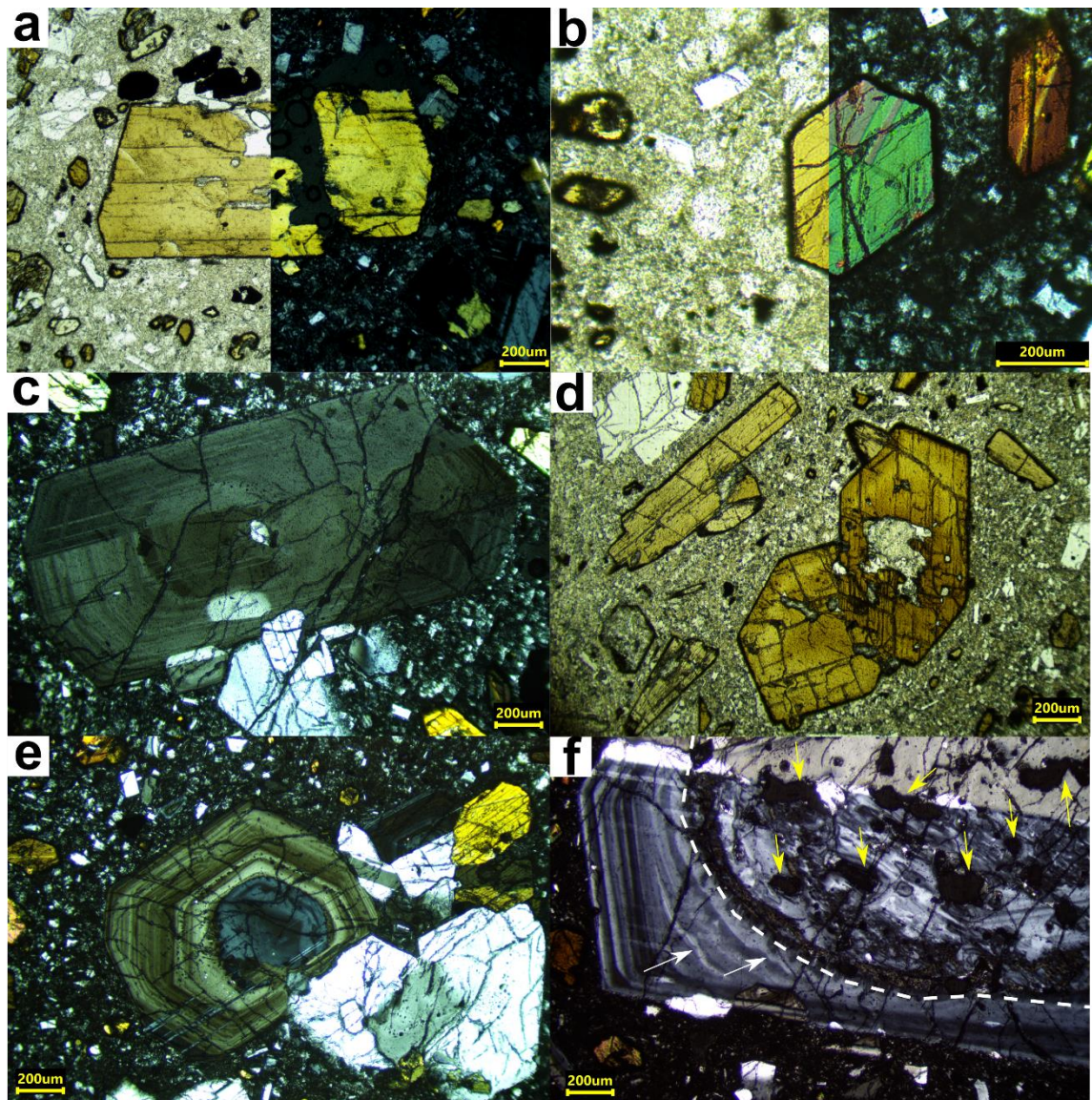


Figure 4.3 Representative photomicrographs of crystals from the post-caldera Cuicocha domes taken with an optical microscope. a) Amphibole phenocryst with thin reaction rim and skeletal texture, sample Yerovi dome (CI3) (right: XPL; left: PPL) b) Euhedral hexagonal microphenocryst of Amp with breakdown rim, sample Yerovi dome (CI3) (right: XPL; left: PPL); c) Oscillatory zoned Pl, sample Yerovi dome (CI3) (XPL); d) Microphenocryst of skeletal Amp, sample Teodoro Wolf dome (CI7) (PPL); e) Oscillatory zoned Pl which presents rounded core, sample Teodoro Wolf dome (CI9) (XPL); f) Patchy zoning core (delineated by white dashed lines) with glass inclusions (indicated by yellow arrows) surrounded by oscillatory zoning with wavy zoning surfaces (indicated by white arrows) in Pl, sample Teodoro Wolf dome (CI7) (XPL).

4.2.7 Enclave in Yerovi dome

Sample CI3 from Yerovi dome contains an enclave with a plutonic texture (Figure 4.4). The enclave present 5% phenocrysts, 35% of microphenocrysts, 5% groundmass with Pl microlites and 55% voids. The phenocrysts are acicular Amp (few hexagonal), with crystals larger than 1 mm presenting a skeletal texture. The microphenocrysts are 20% elongated acicular Amp, 12% Pl and 3% Pxs.

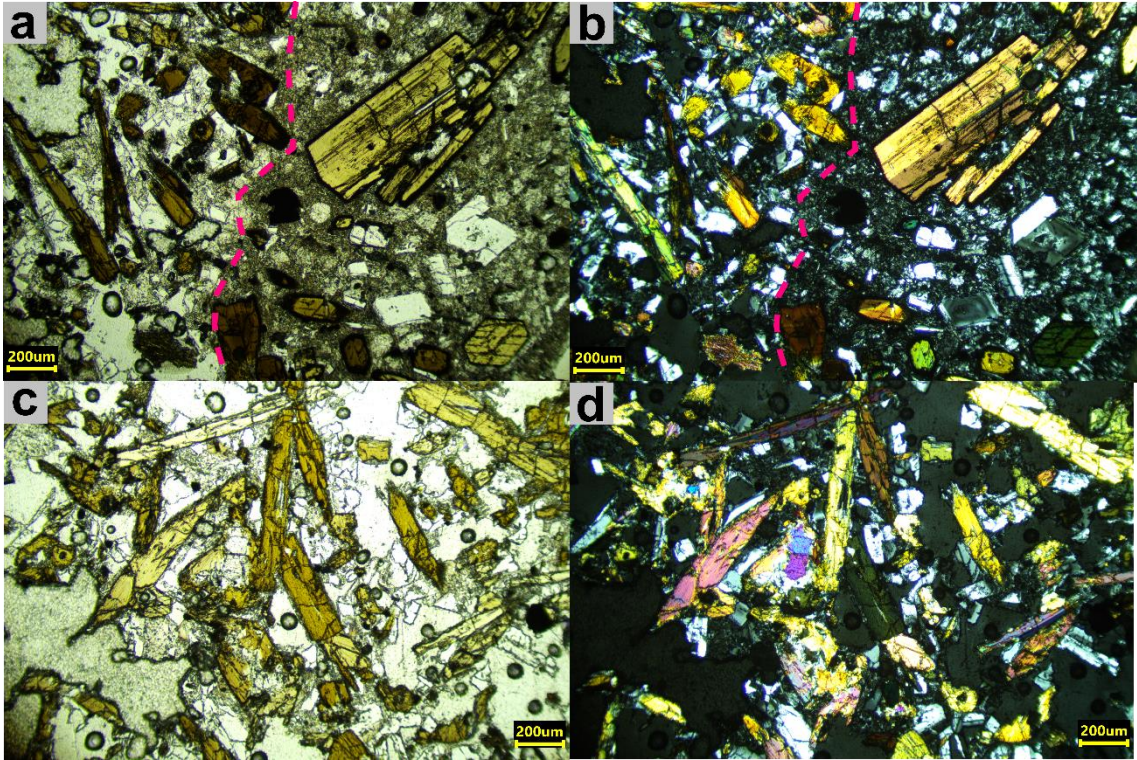


Figure 4.4 Photomicrographs of the limit between the enclave (left) and the host melt (right) in: a) PPL and b) XPL. Note the difference in terms of groundmass and voids between the two. Microphotograph of the enclave in c) PPL and d) XPL.

Table 4.1 Mineral assemblage with percentages (vol %) and textures of the crystals.

Location-Name	Gd (%)	Vs (%)	Phenocrysts (%)				Microphenocrysts (%)					Characteristics
			Amp	Pl	Px	Bt	Amp	Pl	Px	Bt	Opq	
Cotacachi Volcano Lava Flow												
<i>N-shore Cuicocha-CI4</i>	35			3	5			40	15		2	Oz with wavy layers in Pl, Sz in Pl, Tt, Px Glm
<i>Las Antenas-CI6</i>	45		3	2	<1		2	35	10		2	SKt Amp, TKr in Amp (~55 µm), Tt, Px Glm, few zoned Pl
Satellite Domes of the CCVC												
<i>Muyurcu-CI1</i>	15	10		10	10			30	20		5	Pt, few zoned Pl, Glm of just Px and Px with Pl
<i>Loma Negra-CI2</i>	20	10	2	10			8	35	5		10	Pt, SKt Amp, TNr in Amp (~18 µm) some are destroyed and composed of Pl and Px, Px Glm, Oz and SRc in Pl
<i>Peribuela-CI10</i>	33		5	20		2	5	25		8	2	Pt, SKt and TNr (~12 µm) in Amp. Sz and Oz with wavy layers in Pl. Glm of Pl and Amp (alone or both)
Pre-Cuicocha caldera dome												
<i>CI5</i>	25	10	5	35			15	5			5	Pt, SKt and TNr (~15 µm) in Amp. Oz, Pz and SRc in Pl (wavy zoning surfaces) Pl Glm
Post-Cuicocha caldera domes												
<i>Yerovi-CI3</i>	25	10	5	40			10	5			5	Pt, Oz in Pl, TNr (~10 µm) and SKt in Amp. Pl Glm
<i>Enclave in CI3</i>	5	55 voids	5				20	12	3			SKt in Amp
<i>Teodoro Wolf- CI7 and CI9</i>	24	3	5	45			15	5			3	Pt, Glm of Pl and Amp (alone or both), TNr (~12 µm) and SKt in Amp. Oz, Pz, SRc in Pl

Notes: Gd: groundmass; Vs: vesicles; Pz: Patchy zoning; Oz: Oscillatory zoning; SRc: Sub-rounded cores; Sz: Sieve zoning; Tt: Trachyte texture; Pt: Porphyritic texture; Glm: Glomerocrysts; SKt: Skeletal texture; TKr: Thick-reaction rims; TNr: Thin-reaction rims.

4.3 SEM data

Semi-quantitative composition of amphibole's cores and rims from Yerovi, Loma Negra and Cotacachi lava flow (CI6) are presented. The location of these EDS point analyses are shown in Figure 4.5. Moreover, BSE images of Amp rims, Pl and Pxs are described.

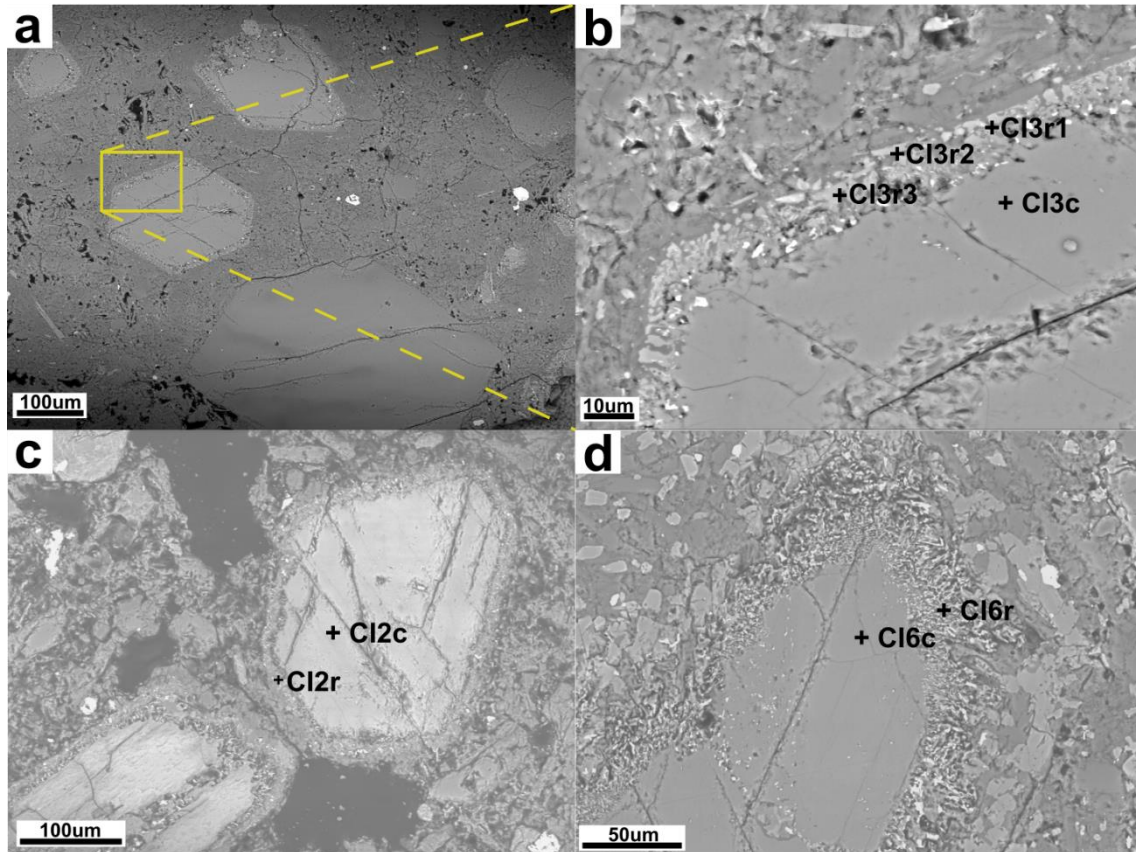


Figure 4.5 SEM images of Amp. Location of rim and core point analysis in amphibole from a) and b) Yerovi dome (CI3); b) Loma Negra (CI2) and c) Cotacachi lava flow (CI6). CI3r: location of rim point analysis in amphibole from Yerovi. CI3c: location of core point analysis in amphibole from Yerovi. CI2r: location of rim analysis in amphibole from Loma Negra. CI2c: location of core point analysis in amphibole from Loma Negra. CI6r: location of rim point analysis in amphibole from Cotacachi lava flow (CI6). CI6c: location of core point analysis in amphibole from Cotacachi lava flow (CI6).

The composition of amphibole's cores in samples from Yerovi dome, Loma Negra dome and Cotacachi lava flow are shown in Table 4.2. Based on the composition the three samples belong to the alkali amphibole group and present variations in composition observed for MgO, Al₂O₃, Fe₂O₃ and SiO₂.

Table 4.2 Compositions of the core of amphiboles obtained by SEM-EDS analysis (in weight %).

Location- Name	Na₂O	MgO	Al₂O₃	SiO₂	K₂O	CaO	TiO₂	Fe₂O₃	Total
Yerovi- CI3c	2.44	12.11	12.68	50.13	0.45	9.51	0.86	11.84	100.02
Loma Negra- CI2c	2.61	13.35	14.95	47.31	0.37	9.66	1.38	10.37	100
Cotacachi lava-CI6c	2.64	14.56	13.66	47.59	0.47	10.34	1.8	8.92	99.98

The composition of the minerals forming the amphibole's rims in samples from Loma Negra dome, Yerovi dome and Cotacachi lava flow are presented in Table 4.3. Our results show that the analyzed minerals forming on the rim of the Amp in the Yerovi sample are Opx with En₆₀₋₆₅Fs₃₂₋₃₅Wo₃₋₆, whereas Cpx is forming on the rim of the Amp in Loma Negra and Cotacachi lava flow samples, with compositions En₅₃₋₅₇Fs₁₅₋₂₅Wo₁₉₋₂₈.

Table 4.3 Compositions of amphibole reaction rims from EDS analysis (in weight %).

Location- Name	Na₂O	MgO	Al₂O₃	SiO₂	K₂O	CaO	TiO₂	Fe₂O₃	Total
Yerovi-CI3r1	1.48	16.53	8.26	55.28	0.36	1.83	0.73	14.87	99.34
Yerovi-CI3r2	1.83	15.43	6.95	57.25	0.42	1.64		15.89	99.41
Yerovi-CI3r3	1.16	17.91	7.11	55.16	0.33	1.47	0.79	15.56	99.49
Loma Negra- CI2r	2.85	1.98	9.89	76.49	1.04	2.61	0.75	4.4	100.01
Cotacachi lava- CI6r	1.25	15.43	9.43	43.96	0.24	10.55	2.79	16.36	100.01

4.3.1 Amphibole rims

The amphibole reaction rims from Loma Negra dome, Yerovi dome and Cotacachi lava flow are composed of Pxs and oxides varying in size from 1 to 10 μ m. Oxides in BSE images are identified as white small areas (blue arrows in Figure 4.6) and pyroxenes as light grey colors (red arrows in Figure 4.6). The Amp phenocrysts from Cotacachi lava

flow have a thick rim (~50 μm). It contains micron-scale oxides which are often elongated, giving a scratched appearance to the rim (Figure 4.6a, 4.6b and 4.6c). Amphibole phenocrysts belonging to the pre-Cuicocha caldera dome present a thin rim (~14 μm), which has very few oxides, circular in shape. Figure 4.6d, shows that towards the core, there is a lighter layer (~5 μm) that is only seen in the upper part of the amphibole crystal. Amphibole microphenocryst from Loma Negra dome present a rim rich in oxides. The rim is approximately 20 μm thick; however, it varies in thickness. The rim is formed by two identifiable layers; the layer one (L1) is the outside layer and is lighter than layer 2 (L2). L2 contains more oxides than L1, however the oxides from L1 are euhedral and bigger (Figure 4.6e and 4.6f). L1 layer is similar to the Amp rim of the pre-Cuicocha caldera dome. Amphibole microphenocryst from Yerovi dome also present a thin rim containing less oxides than Loma Negra and anhedral in shape. The thickness of the rim is ~13 μm , almost constant thickness. This reaction rim is similar to L2 in Loma Negra Amp; however, the shape of the oxides is anhedral in this case (Figure 4.6g and 4.6h).

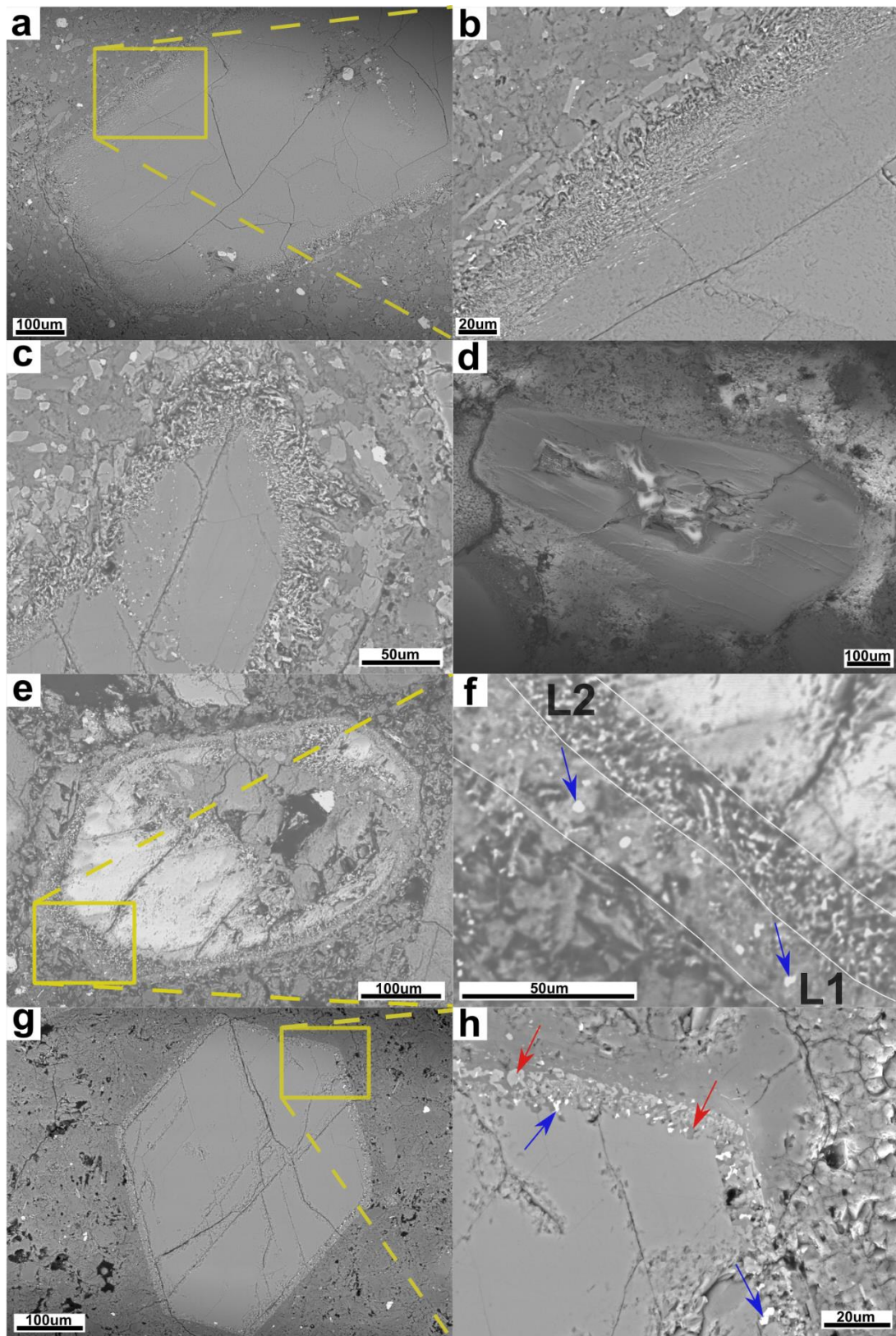


Figure 4.6 SEM images of amphiboles. a) Microphotographs of Amp from the Cotacachi lava flow (CI6); b) Detailed image of the reaction rim of Amp in a); c) Microphotograph of another Amp from the Cotacachi lava flow (CI6); d) Microphotograph of Amp from the pre-Cuicocha caldera dome (CI5); e) Microphotograph of Amp from Loma Negra dome (CI2); f) Detailed microphotograph of e) amphibole rim showing two different layers; g) Microphotograph of Amp belonging to Yerovi dome (CI3); h) Detailed microphotograph of Amp rim of g). Blue arrows point some oxides and red arrows point some Pxs.

4.3.2 Plagioclase zoning and texture

Plagioclase photomicrographs from Loma Negra and pre-Cuicocha caldera dome are presented in Figure 4.7. As shown in Figure 4.7a, some Pl microphenocryst from Loma Negra present a patchy Na-rich core with a thin Ca-rich rim (~17 μm). The core also presents calcic Pl growth after dissolution of the initial Pl. Pl phenocryst from pre-Cuicocha caldera dome (Figure 4.7b) presents a patchy Na-rich plagioclase with calcic Pl growth as in Loma Negra Pl microphenocryst. Moreover, it is possible to identify a sub-rounded sieve zone (yellow dashed lines) with glass inclusions (dark points within the area delineated with the yellow dashed lines).

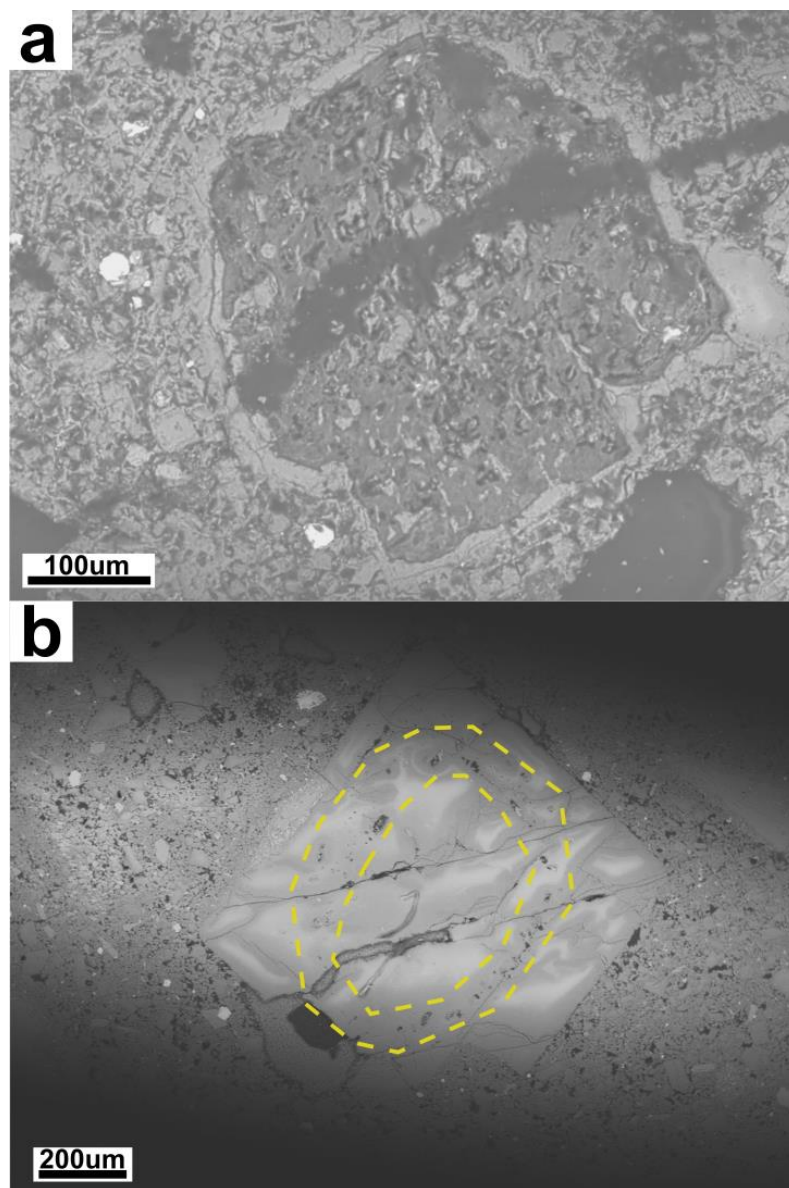


Figure 4.7 Microphotographs of Pl from: a) Loma Negra dome (CI2); b) Pre-Cuicocha Caldera dome. Different grey scale color represents different composition. Light grey: Ca-rich zones; dark grey: Na-rich zones.

4.3.3 *Pyroxenes zoning*

SEM images of Px are presented in Figure 4.8, demonstrating light grey color representative of low Mg content, whereas dark grey color reflects high Mg content within Px. Figures 4.8a show zonation in Px from Muyurcu dome (CI1), including the core (zone 1 in Figure 4.8a) and two extra zones that are a lighter outer zone (zone 3 in Figure 4.8a) and a darker (zone 2 in Figure 4.8a). The thicknesses of the zones vary in each crystal. In Figure 4.8b, is shown a Px microphenocryst from Cotacachi lava flow (CI6) that also presents zoning, consisting the core (zone 4 in Figure 4.8b) and two zones (zone 5 and 6 in Figure 4.8b). In this case the outer zone is the darker and is not present all around the crystal, while the next zone (zone 5 in Figure 4.8b) is the lighter.

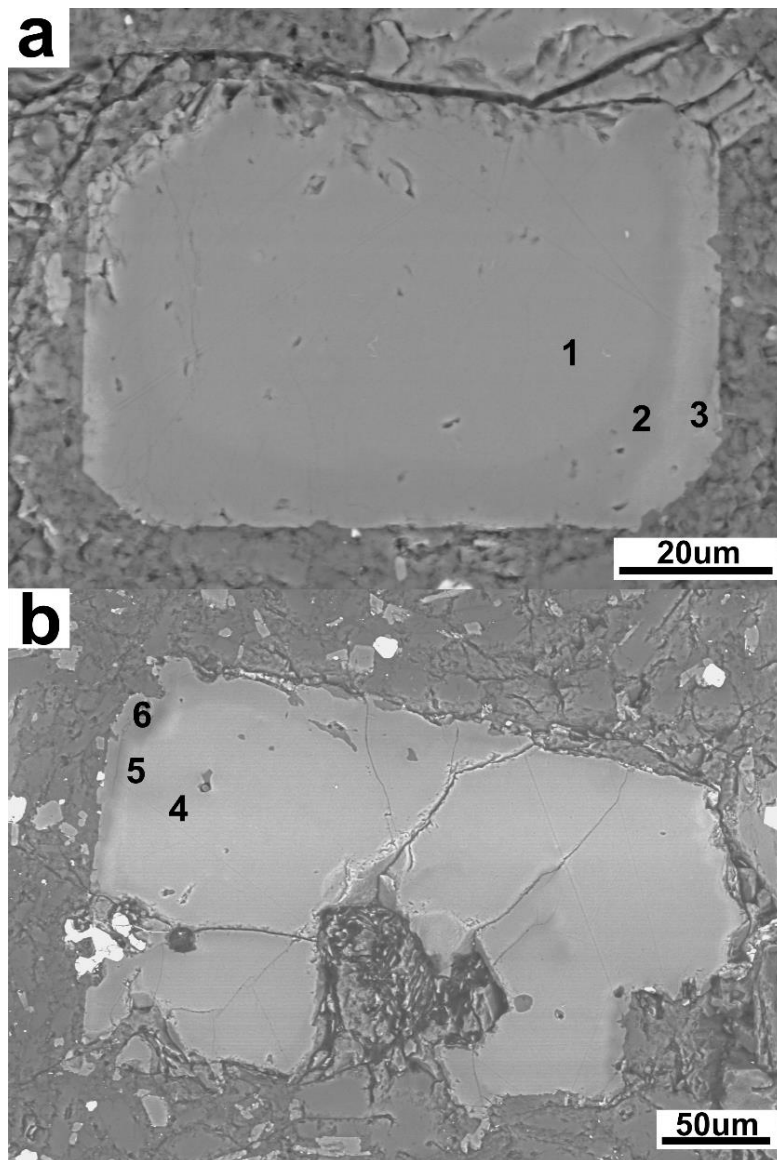


Figure 4.8 Microphotographs of different Px showing zonation pattern from: a) and b) Muyurcu dome; c) Cotacachi lava flow (CI6)

4.3.4 Enclave in Yerovi dome

Figure 4.9a shows the sharp contact between the enclave and the host. The enclave presents a plutonic texture and a lot of voids (dark areas), which are not considered vesicles due to their shape. In fact, vesicles usually have smooth and rounded walls, however in Figure 4.9b it is possible to see that the dark areas are filling all the spaces between the crystals and do not present rounded walls. Moreover, Amp microphenocrysts in the enclave, which are touching each other, do not present reaction rim as was seen in Amp from the host rock.

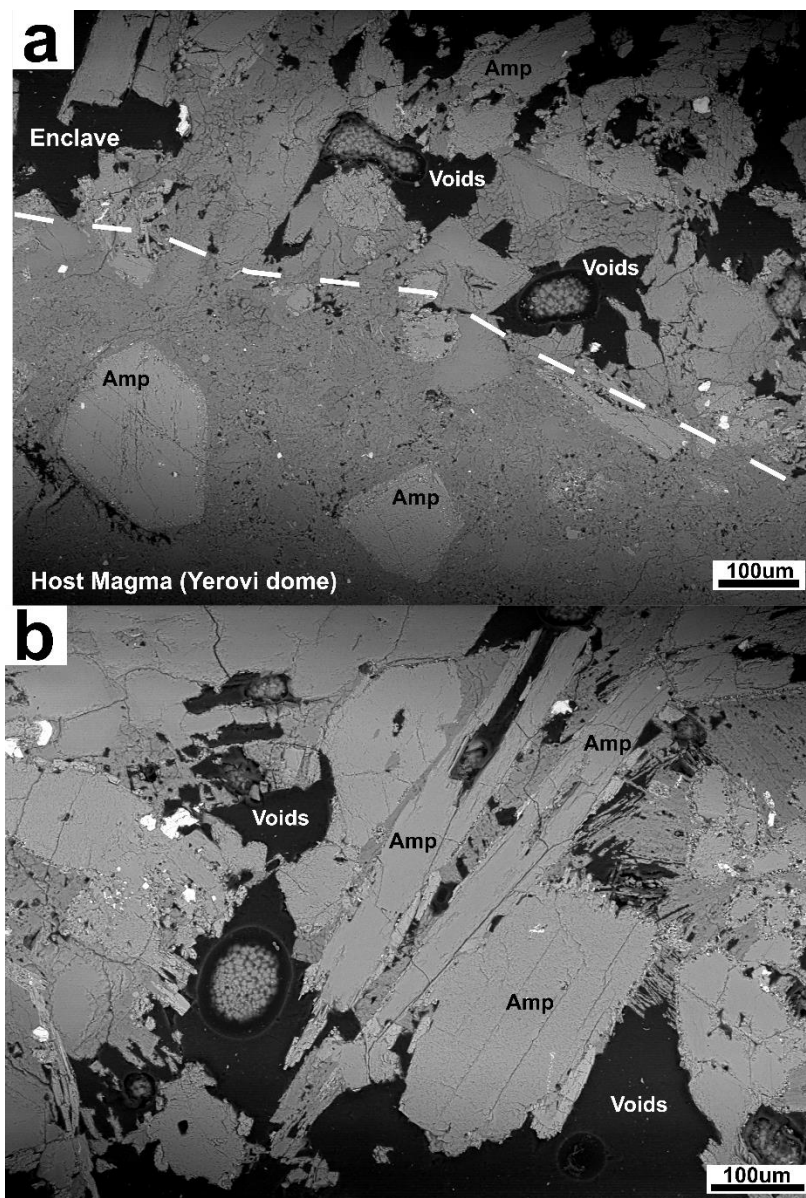


Figure 4.9 Microphotographs of: a) limit between the enclave and the host magma of Yerovi dome; and b) Acicular Amp of the enclave without reaction rims. Note the shape of the voids in the enclave, breaking crystals apart.

CHAPTER 5: DISCUSSION

The main differences between crystals of the rocks from the CCVC are the thickness and composition of Amp rims, the textures in Pl, and the compositional zoning in Pxs and Pl. These features observed in crystals are proper evidence of heating due to magma mixing, kinetic movement of crystals, decompression in the magmatic system and different chemical composition of the magma associated with this volcanic complex.

5.1 *Amphibole rims*

The composition of the rim is a good indicator of the process/es to which the amphibole was subjected. Rims with Opx occur due to decompression, whereas rims with Cpx are produced by heating due to interaction with hotter magma (Browne, 2005). Sample from Yerovi dome (CI3) contains Opx in its Amp rim, that can be interpreted as a result of decompression process. In contrast, the presence of Cpx in the Amp rim of samples from Loma Negra (CI2) and Cotacachi lava flow (CI6) can be advocated to be formed by heating during magma mixing. However, more analysis of each of the rims would yield more confidence in the previous statement. Moreover, more characteristics of the amphibole rims have to be taken into account to be able to identify the process to which Amp were subjected. In addition, according to Browne (2005), if the Amp was subjected to a multi-step isothermal decompression at 10 MPa/day, the average thickness of the rim should be ~15 μm and the composition fine-grained (~2 μm) Opx and Pl with trace amounts titanomagnetite. Likewise, the average ~13 μm thickness of the rim and occurrence of fine-grained Opx with few amounts of oxides observed in Amp rim of Yerovi sample, can support the decompression process.

On the other hand, recent experiments carried out by Angelis et al. (2015) demonstrated that rims than contain only Opx can be the result of either decompression or heating. Therefore, the thickness of the reaction rim can assist to interpret the induced processes. Thus if the amphibole was subjected to heat for some time, the rim will grow 10-100 times faster than rims produced by a decompression process, whereas if the amphibole was subjected to decompression the thickness would be less (Browne, 2005). Accordingly, Yerovi dome Amp rim can be interpreted to be formed by decompression-induced process due to the thinner rims (~13 μm). The Amp rim from Cotacachi lava flow can be inferred to be generated via heating-induced process, having rims with ~50

μm thickness, which is in agreement with experimental work done by Browne (2005). Moreover, amphibole rim from Loma Negra, showing $\sim 20 \mu\text{m}$ thickness, which can be considered as heating-induced but shortly prior to the eruption, that is why their rims are not as thick as in Amp phenocrysts from Cotacachi lava flow.

Viscosity, which is defined as the resistance to flow, is dependent on temperature, pressure, magma composition among others. Decompression, for instance, causes an increase in melt viscosity whereas an increase in temperature reduces it (Angelis et al., 2015). So, given that for Cotacachi lava flow (CI6), the process that formed the amphibole rim was established as heating-induced, therefore, the viscosity of the melt should be reduced. This is consistent with the fact that this sample belongs to a melt that was able to flow and has low crystal content if we just take into account the phenocrysts ($<10\%$). It is important to mention that only the phenocrysts are considered because it is possible that the magma, as it ascends, only contains phenocrysts and that the microphenocrysts were created during and after emplacement of the lava flow (Cashman et al., 1999). Following the relationship between viscosity and temperature proposed by Angelis et al. (2015), melt from Loma Negra dome should have experienced a decrease in viscosity due to heating, the process that caused the reaction rims in Amp. However, this magma was still very viscous when it reached the surface as it formed a dome. Thus, we suggest that the melt before the mixing process was cold and viscous with Amp and Pl phenocrysts. However, when the heating occurred, the Amp reaction rims grew and the viscosity decreased. The Pxs microphenocrysts (5%) present in Loma Negra rock sample either grew after the mixing or were transported from the hotter and more mafic magma. The ratio of hot to cold magma was thus enough to induce reaction rims and Px phenocrysts growth, but not enough to lower the viscosity of the whole reservoir. In the case of Yerovi dome, the decompression process that provoked the reaction rim in Amp also increased the viscosity of the melt allowing the formation of a dome.

Additionally, the thickness of amphibole rims also appears to be a function of magma ascent rate from a deep source, so thin-rimmed Amp ascended faster than thicker-rimmed Amp (Buckley et al., 2006). Hence, the thin rims of Amp microphenocrysts from Yerovi dome suggest that the melt rised fast. This is also supported by the vesicles observed in this sample. About 10% of vesicles is estimated in Yerovi dome sample, which shows

that the gases were not able to completely separate from the magma due to a fast ascent of the melt (Cashman, 2004).

5.2 *Plagioclase zoning and texture*

Viccaro et al. (2010) interpreted that oscillatory zoning in plagioclase is due to kinetics effects at the plagioclase/melt interface or crystallization in a dynamic regime driven by chemical and physical gradients. In the same way, Troll et al. (2004) argues that this type of zoning is the result of long-term processes that are prevalent in the system instead of high impact events. According to these interpretations and given that all of the rock samples present at least one oscillatory zoned Pl, the magmatic system of the CCVC could have experienced long-term processes that enhance the movement of the crystals inside the magmatic system.

Moreover, Jeffery et al. (2013) suggested that dissolution and crystal kinetics are the main cause of the wavy zoning surfaces in oscillatory zoning. Besides, Frey and Lange (2011), and Ginibre et al. (2002) proposed that these resorptions surfaces could be caused by the movement of the magma within the system, heating and/or decompression with no fluid involved. These wavy surfaces in oscillatory zoning (Figure 4.2f, 4.2h, 4.3e, 4.3f) are very evident in Pl (phenocrysts and microphenocrysts) from all the rocks samples, except Muyurcu dome, suggesting that crystals from the magmatic system of the CCVC were subjected to dissolution, movement, heating and/or decompression. Furthermore, some Pl from Loma Negra, pre-Cuicocha caldera and Teodoro Wolf domes present sub-rounded embayed cores which represent minor dissolution in a crystal surrounded by a hotter melt of different composition (Renjith, 2014). Pre-Cuicocha caldera and Teodoro Wolf domes have Pl with patchy zones which form due to decompression in magmas undersaturated in water (Humphreys et al., 2006; Renjith, 2014; Vance, 1965; Viccaro et al., 2010). Plagioclase from Peribuela dome present sieve textures which are the result of the interaction of plagioclase with a more mafic and/or hotter and Ca-rich melt in which An-rich Pl is in equilibrium (Humphreys et al., 2006; Renjith, 2014). In the same way, by analyzing Loma Negra Pl microphotograph (Figure 4.7a), it is possible to conclude that this crystal also underwent a mafic magma recharge in the magma chamber due to the presence of an abrupt Ca-rich overgrowth rim which indicates a disequilibrium condition that returns to a less evolved compositions (Ginibre et al., 2007).

5.3 *Pyroxene zoning*

Pyroxene (phenocrysts and microphenocrysts) from Muyurcu and Cotacachi lava flow (CI6) demonstrate that mixing took place during the last stage of their growth due to the presence of different greyscale zones that reflect variations in composition. For example, light areas show that the mineral grows in a cooler and more evolved magma with low Mg#, and dark grey areas demonstrate that the crystal grows in a hotter and more mafic magma rich in Mg# (Frey and Lange, 2011; Gagnevin et al., 2007; Petrone et al., 2018). Knowing this, Px microphenocrysts (Figure 4.8a) from Muyurcu dome started to grow in a low Mg# magma. Then, after an interaction with hotter and more mafic magma responsible for the darker layer, fractional crystallization resulted in an evolved and Fe-rich magma in which Px developed their outer rims. In the case of Cotacachi lava flow, Px microphenocryst started to grow in a low Mg# magma; as Px microphenocrysts from Muyurcu, the cooling and the crystallization continued resulting in a magma more evolved and richer in Fe. Lastly, a hotter and high Mg# magma produces the dark-grey rims visible in Figure 4.8b.

5.4 *Enclave in Yerovi dome*

The enclave observed in Yerovi dome has Px, Amp and Pl, while the host melt has Amp and Pl. The empty spaces between crystals, the shape of these spaces (elongated), the contact between minerals, the lack of groundmass (~5%) and the fractured-like texture suggest that the enclave could be a part of a crystal mush incorporated within this magma on the move. Crystal mush is a mixture of crystals (>40% vol) and liquid (Cooper, 2017) that is formed in a system where the dense particles settle at the bottom of the reservoir (Bachmann and Bergantz, 2008). In this case, the crystal mush could be a remnant of a previous unerupted magma left in the magmatic reservoir, and the melt that formed Yerovi dome ripped off parts of this crystal mush during its ascent carrying it to the surface.

5.5 *Viscosity, crystal content (size and modal abundance) and vesicles*

Viscosity of a magma is affected by volatiles, crystal and silica content. A magma containing fewer crystals can easily flow, whereas a magma with a significant amount of crystals would not flow easily (Németh and Martin, 2007). Regarding our samples, it is possible to note that the lava flows from Cotacachi volcano have ~60 vol % of crystals, which seems to be a high percentage for lavas to flow. However, it is important to take

into account that some crystals nucleate during flowing of the lava due to stirring of the flow and grow when the magma cools quickly, at the surface (Cashman et al., 1999). Thus, most of the microphenocrysts, <700 μm in size, which account for ~50 %, may have been created during cooling and emplacement on the surface after the eruption of both of the lava flows. In the case of pre- and post-Cuicocha caldera domes, they present the highest percentage of phenocrysts (~50 %) and the lowest percentage of microphenocrysts of the volcanic complex. This gives the idea that magma from Cuicocha (pre- and post-caldera domes) spent more time in the magma chamber where the crystals were able to grow. For Loma Negra, Peribuela and Muyurcu dome the percentage of microphenocrysts is the highest, ~55 %, showing that the nucleation rate of these crystals in the melt was higher than pre- and post-caldera domes which have ~20 % of microphenocrysts.

In terms of vesicles, the lava flow samples do not present them, while domes have 10 %. Knowing, that crystallization increases volatile content and favors nucleation of bubbles, and that less viscous melt can degas more efficiently than their viscous counterpart (Sigurdsson et al., 2015 and references therein), the higher vesicularity of dome samples compared to lava flows is logical. However, for Peribuela, this does not match, given that this dome is the only one that does not have vesicles. This could be explained by the fact that melt associated with Peribuela ascended slower than melt from the other domes, which allowed the gases to escape, or the volatile content of the melt of Peribuela was lower compared to that of the other domes.

5.6 Interpretation of the magmatic history of each volcanic center

CI4 sample from the Cotacachi lava flow is considered the first emplacement of all the rock samples studied here even if it was collected far from the summit of the volcano comparing to the other lava flow sample (CI6). This statement to establish CI4 lava flow as the older rock is based on the facts that this rock sample was covered by ~100 m of younger deposits and that at the beginning, there could be a smooth topography, which allowed that CI4 lava flows easily far away. Additionally, this rock sample is more mafic (Pl and Pxs) than CI6 (Amp, Pl and Pxs), so the magma was less viscous, allowing it to flow further.

In Muyurcu dome, which is 138 ± 4 ka (Bablon, 2019), the melt was colder and more evolved than CI6 lava flow, which allowed the crystallization of more Pxs rich in Fe;

however, an influx of hotter and mafic magma, recorded by zoning of Pxs microphenocrysts, occurred. Finally, fractional crystallization continued increasing viscosity, decreasing temperature and preventing movement of the magma within the chamber that is reflected in the lack of wavy zoning surfaces in oscillatory zoning of Pl. This viscous melt was not able to flow and formed Muyurcu dome.

For CI6 Cotacachi lava flow, that is 108 ± 4 ka (Almeida, 2016), the melt within the reservoir was more evolved and cold, allowing the crystallization of Amp and Pxs rich in Fe, then an influx of hotter and mafic magma occurred provoking dark grey rims in Pxs microphenocrysts and destabilizing the Amp forming its rims. Due to the influx of this new hot magma, the viscosity decreased, which could end up with the eruption of CI6 lava flow.

For Loma Negra the magmatic system was colder and Na-rich Pl microphenocrysts crystallized; however, an influx of hotter mafic magma occurs, provoking that Amp developed dark reaction rims, and Pl Ca-rich rims. Nevertheless, the amount of the intruded magma must have been little, which is suggested by the thin reaction rims developed and the high viscosity of the magma that formed a dome rather than flow.

In Peribuela dome the melt in the reservoir was cold and evolved, allowing the crystallization of Bt. However, an influx of more mafic and/or hotter and Ca-rich magma recorded by the presence of sieve texture in Pl and reaction rim in Amp occurred and possibly triggered the emplacement of this dome.

For pre-Cuicocha caldera dome, it is suggested that before its emplacement, there was a considerable time lapse where Pl (Na-rich) and Amp phenocrysts were able to grow and circulate in the magmatic gradient inside the reservoir. Decompression was recorded by Amp through the growth of reaction rims; and the patchy zones in Pl, which also evidences a magma undersaturated in water. Recharge of magma, which was recorded by the dissolution of Na-rich Pl and growth of Ca-rich Pl, ultimately resulted in a more mafic magma (Pl and Amp) than the one which formed Peribuela dome (Pl, Amp and Bt). This magma mixing could be the process that triggered the emplacement of the pre-Cuicocha caldera dome. For post-Cuicocha caldera domes, the presence of patchy zones in plagioclase and reaction rims in Amp, suggest that decompression occurred too. Furthermore, given that pre- and post-Cuicocha caldera domes have very similar modal

abundances of phenocrysts and microphenocrysts and were emplaced at the same location, they could form from a similar magma source.

Finally, based on previous rock dating (Almeida, 2016; Bablon, 2019) and relative age based on stratigraphy proposed by Von Hillebrandt (1989) and Pidgen (2014), CI4 lava flow was first, then Muyurcu dome, CI6 lava flow, Loma Negra, Peribuela, pre-Cuicocha caldera dome and, finally, the post-Cuicocha caldera domes. However, between and during these events, many processes within the magmatic plumbing system could occur confirming the fact that the CCVC is a very complex system in which one big reservoir could be the source of magma or many magmatic batches located at different depths could exist as the sources for different eruptive phases.

CHAPTER 6: CONCLUSIONS

Crystals of the different rocks from the CCVC were able to record some of the processes that occurred within the magmatic reservoir(s) throughout the history of this volcanic complex. The processes identified by analyzing textures and zoning in Amp, Pl and Pxs, were decompression, movement of crystals within the reservoir and intrusion of hotter and more mafic magma, i.e. magma mixing. Moreover, some physical properties of the magma, such as viscosity, crystal, and volatile content were analyzed by characterizing crystal population, their modal abundances and vesicles. In this way, it was possible to reconstruct the magmatic history of the different eruptive phases of the CCVC by knowing the processes that occurred in depth for each dome.

Moreover, knowing that the CCVC has presented throughout its history different eruptive styles from lava flows to dome growing and formation of calderas, this study pretends to raise awareness of the risk associated with this volcanic complex. For example, the growth of domes could be considered less risky than a lava flow that can travel for some kilometers. However, if the dome collapse and produce PDCs, the risk increases significantly. Additionally, a climactic eruption such as the one that destroyed the pre-Cuicocha caldera dome and led to the formation of the caldera may affect many more people and cause damage to infrastructure, being this an important issue to consider. By considering the active volcanic context of Ecuador, this study pretends to raise the consciousness of people, especially authorities, about the hazard associated to the Cuicocha volcano. Moreover, keeping improving hazard preparedness of populations near CCVC and monitoring systems of this volcanic complex, is essential to safeguard people's lives who visit Cuicocha lake and live near CCVC.

This study shows how powerful is a petrographic study to reveal processes that occurred in magmatic systems. However, it is important to mention that quantitative analyses are needed to understand better the evolution of the magma of this volcanic complex. Future studies could include XFR and ICP-MS for major and trace element analysis of the different units to better understand chemical evolution of the magmas. EPMA would provide more precise analysis of reaction rims, zoned crystals and mineral composition in general while cathodoluminescence (CL) images would allow to see in detail growth or resorption textures. Dating of the lava flows and domes would also be beneficial to reconstruct the history of the CCVC.

REFERENCES

- Almeida, M., 2016. Estudio Petrográfico y Geoquímico del Volcán Cotacachi - Provincia de Imbabura. Ecuador. Undergraduate Thesis. Escuela Politecnica Nacional. <https://doi.org/10.13140/RG.2.2.19884.46727>
- Angelis, S.H. De, Larsen, J., Coombs, M., Dunn, A., Hayden, L., 2015. Amphibole reaction rims as a record of pre-eruptive magmatic heating: An experimental approach. *Earth Planet. Sci. Lett.* 426, 235–245. <https://doi.org/10.1016/j.epsl.2015.06.051>
- Aspden, J., McCourt, W., Brook, M., 1987. Geometrical control of subduction-related magmatism: the Mesozoic and Cenozoic plutonic history of Western Colombia. *J. Geol. Soc. London.* 144, 893–905.
- Bablon, M., 2019. Reconstruction de l'histoire des volcans de l'arc équatorien: contraintes pour l'évolution chronologique de l'arc andin et pour l'évaluation du risque volcanique. PhD Thesis. Université Paris-Saclay.
- Bachmann, O., Bergantz, G., 2008. The magma reservoirs that feed supereruptions. *Elements* 4, 17–21. <https://doi.org/10.2113/GSELEMENTS.4.1.17>
- Barker, A.J., 2014. A Key for Identification of Rock-forming Minerals in Thin-Section. CRC Press, University of Southampton, UK.
- Blundy, J., Cashman, K., 2008. Petrologic reconstruction of magmatic system variables and processes. *Rev. Mineral. Geochemistry* 69, 179–239. <https://doi.org/10.2138/rmg.2008.69.6>
- Browne, B.L., 2005. Petrologic and Experimental Constraints on magma mingling and ascent: Examples from Japan and Alaska. PhD Thesis. University of Alaska Fairbanks.
- Buckley, V.J.E., Sparks, R.S.J., Wood, B.J., 2006. Hornblende dehydration reactions during magma ascent at Soufrière Hills Volcano, Montserrat. *Contrib. to Mineral. Petrol.* 151, 121–140. <https://doi.org/10.1007/s00410-005-0060-5>
- Bustos Gordón, E.A., Serrano, N.L., 2014. Análisis de la distribución espacial de la emisión difusa de CO₂ en las calderas volcánicas Cuicocha y Quilotoa, como sustento técnico para la toma de decisiones en la gestión de riesgos. Undergraduate

Thesis. Universidad de las Fuerzas Armadas ESPE.

- Cashman, K., Thornber, C., Kauahikaua, J., 1999. Cooling and crystallization of lava in open channels, and the transition of Pahoehoe Lava to 'A'a". *Bull. Volcanol.* 61, 306–323. <https://doi.org/10.1007/s004450000090>
- Cashman, K. V., 2004. Volatile controls on magma ascent and eruption. *Geophys. Monogr. Ser.* 150, 109–124. <https://doi.org/10.1029/150GM10>
- Cooper, K.M., 2017. What does a magma reservoir look like? the “crystal’s-eye” view. *Elements* 13, 23–28. <https://doi.org/10.2113/gselements.13.1.23>
- Cordero, M., Amonte, C., Melián, G. V, Toulkeridis, T., Alonso, M., Bustos, A., Padrón, E., Asensio Ramos, M., Hernández, P.A., Pérez, N.M., 2019. Monitoring CO2 emission from Cuicocha Volcanic Lake, Ecuador., in: *Geophysical Research Abstracts* (Vol. 21).
- Córdova, A., Ruiz, M., Villarreal, E., Hidalgo, S., Yépez, M., 2018. Informe Especial N°02 –2018.Volcán Cuicocha."Actualización del Estado de Actividad Sísmica: Retorno al Nivel de Base.
- Costa Rodriguez, F., Chakraborty, S., Dohmen, R., 2003. Diffusion coupling between trace and major elements and a model for calculation of magma residence times using plagioclase Diffusion coupling between trace and major elements and a model for calculation of magma residence times using plagioclase. *Geochim. Cosmochim. Acta* 67, 2189–2200. [https://doi.org/10.1016/S0016-7037\(00\)01345-5](https://doi.org/10.1016/S0016-7037(00)01345-5)
- Frey, H.M., Lange, R.A., 2011. Phenocryst complexity in andesites and dacites from the Tequila volcanic field, Mexico: Resolving the effects of degassing vs. magma mixing. *Contrib. to Mineral. Petrol.* 162, 415–445. <https://doi.org/10.1007/s00410-010-0604-1>
- Gagnevin, D., Waight, T.E., Daly, J.S., 2007. Insights into magmatic evolution and recharge history in Capraia Volcano (Italy) from chemical and isotopic zoning in plagioclase phenocrysts Insights into magmatic evolution and recharge history in Capraia Volcano (Italy) from chemical and isotopic z. *J. Volcanol. Geotherm. Res.* 168, 28–54. <https://doi.org/10.1016/j.jvolgeores.2007.07.018>
- Ginibre, C., Wörner, G., Kronz, A., 2002. Minor- and trace-element zoning in

- plagioclase: Implications for magma chamber processes at Parinacota volcano, northern Chile. *Contrib. to Mineral. Petrol.* 143, 300–315. <https://doi.org/10.1007/s00410-002-0351-z>
- Ginibre C, Wörner G, Kronz A, 2007. Crystal Zoning as an Archive for Magma Evolution. *Elements* 3, 261–266.
- Goldstein, Joseph Newbury, D.E., Echlin, P., Joy, D., Lyman, C.E., Lifshin, J.R., 2003. Scanning electron microscopy and X-ray microanalysis, Third. ed. Kluwer Academic/Plenum.
- Gunkel, G., Beulker, C., 2009. Limnology of the crater lake cuicocha, ecuador, a cold water tropical lake. *Int. Rev. Hydrobiol.* 94, 103–125. <https://doi.org/10.1002/iroh.200811071>
- Gunkel, G., Beulker, C., Grupe, B., Gernet, U., Viteri, F., 2011. Aluminium in Lake Cuicocha, Ecuador, an Andean Crater Lake: Filterable, Gelatinous and Microcrystal Al Occurrence. *Aquat. Geochemistry* 17, 109–127. <https://doi.org/10.1007/s10498-010-9114-z>
- Gunkel, G., Beulker, C., Grupe, B., Viteri, F., 2009. Survey and assessment of post volcanic activities of a young caldera lake, Lake Cuicocha, Ecuador. *Nat. Hazards Earth Syst. Sci.* 9, 699–712. <https://doi.org/10.5194/nhess-9-699-2009>
- Gunkel, G., Beulker, C., Grupe, B., Viteri, F., 2008. Hazards of volcanic lakes: Analysis of Lakes Quilotoa and Cuicocha, Ecuador. *Adv. Geosci.* 14, 29–33. <https://doi.org/10.5194/adgeo-14-29-2008>
- Hall, M.L., Samaniego, P., Le Pennec, J.L., Johnson, J.B., 2008. Ecuadorian Andes volcanism: A review of Late Pliocene to present activity. *J. Volcanol. Geotherm. Res.* 176, 1–6. <https://doi.org/10.1016/j.jvolgeores.2008.06.012>
- Hall, M.L., Wood, C.A., 1985. Volcano-tectonic segmentation of the northern Andes. *Geology* 13, 203–207. [https://doi.org/10.1130/0091-7613\(1985\)13<203:VSOTNA>2.0.CO;2](https://doi.org/10.1130/0091-7613(1985)13<203:VSOTNA>2.0.CO;2)
- Hormann, P.K., Pichler, H., 1982. Geochemistry, Petrology and Origin of the Cenozoic Volcanic Rocks of the Northern Andes in Ecuador. *J. Volcanol. Geotherm. Res.* 12, 259–282. [https://doi.org/https://doi.org/10.1016/0377-0273\(82\)90029-4](https://doi.org/10.1016/0377-0273(82)90029-4)

- Humphreys, M.C.S., Blundy, J.D., Sparks, R.S.J., 2006. Magma evolution and open-system processes at Shiveluch Volcano: Insights from phenocryst zoning. *J. Petrol.* 47, 2303–2334. <https://doi.org/10.1093/petrology/egl045>
- James, D., 1971. Plate tectonic model for the evolution of the Central Andes. *Geol. Soc. Am. Bull.* 82, 3325–3346.
- Jeffery, A.J., Gertisser, R., Troll, V.R., Jolis, E.M., Dahren, B., Harris, C., Tindle, A.G., Preece, K., O'Driscoll, B., Humaida, H., Chadwick, J.P., 2013. The pre-eruptive magma plumbing system of the 2007-2008 dome-forming eruption of Kelut volcano, East Java, Indonesia. *Contrib. to Mineral. Petrol.* 166, 275–308. <https://doi.org/10.1007/s00410-013-0875-4>
- Jerram, D.A., Martin, V.M., 2008. Understanding crystal populations and their significance through the magma plumbing system. *Geol. Soc. Spec. Publ.* 304, 133–148. <https://doi.org/10.1144/SP304.7>
- Lofgren, G., 1974. An experimental study of plagioclase crystal morphology; isothermal crystallization. *Am. J. Sci.* 274, 243–273. <https://doi.org/10.2475/ajs.274.3.243>
- Melián, G. V, Bustos, A., Alonso, M., Toulkeridis, T., Padrón, E., Asensio Ramos, M., Amonte, C., Vela, V., Hernández, P.A., Pérez, N.M., 2018. Carbon dioxide emission from Cuicocha Volcanic Lake, Ecuador., in: EGU General Assembly Conference Abstracts. p. 7389.
- Németh, K., Martin, U., 2007. *Practical Volcanology - Lecture Notes for Understanding Volcanic Rocks from Field Based Studies*, Occasional Papers of the Geological Institute of Hungary. Geological Institute of Hungary.
- Padrón, E., Hernández, P.A., Toulkeridis, T., Pérez, N.M., Marrero, R., Melián, G., Virgili, G., Notsu, K., 2008. Diffuse CO₂ emission rate from Pululahua and the lake-filled Cuicocha calderas, Ecuador. *J. Volcanol. Geotherm. Res.* 176, 163–169. <https://doi.org/10.1016/j.jvolgeores.2007.11.023>
- Pallares, C., Quidelleur, X., Debreil, J.A., Antoine, C., Sarda, P., Tchilinguirian, P., Delpech, G., Gillot, P.Y., 2019. Quaternary evolution of the El Tromen volcanic system, Argentina, based on new K-Ar and geochemical data: Insights for temporal evolution of magmatic processes between arc and back-arc settings. *J. South Am. Earth Sci.* 90, 338–354. <https://doi.org/10.1016/j.jsames.2018.12.022>

- Petrone, C.M., Braschi, E., Francalanci, L., Casalini, M., Tommasini, S., 2018. Rapid mixing and short storage timescale in the magma dynamics of a steady-state volcano. *Earth Planet. Sci. Lett.* 492, 206–221. <https://doi.org/10.1016/j.epsl.2018.03.055>
- Pidgen, A., 2014. Cuicocha Volcano , Ecuador : reconstruction of major explosive phases through investigation of associated pyroclastic deposits. Masters thesis. University of Oxford.
- Pindell, J., Kennan, L., 2009. Tectonic evolution of the Gulf of Mexico, Caribbean and northern South America in the mantle reference frame: an update. *Geol. Soc. London, Spec. Publ.* 328, 1.1-55. <https://doi.org/http://dx.doi.org/10.1144/SP328.1>
- Pourkhorsandi, H., Mirnejad, H., Raiesi, D., Hassanzadeh, J., 2015. Crystal size and shape distribution systematics of plagioclase and the determination of crystal residence times in the micromonzogabbros of Qisir Dagh, SE of Sabalan volcano (NW Iran). *Geol. Carpathica* 66, 257–268. <https://doi.org/10.1515/geoca-2015-0024>
- Reed, S.J., 2005. *Electron Microscope Analysis and Scanning Electron Microscopy in Geology*. Cambridge University Press.
- Renjith, M.L., 2014. Micro-textures in plagioclase from 1994-1995 eruption, Barren Island Volcano: Evidence of dynamic magma plumbing system in the Andaman subduction zone. *Geosci. Front.* 5, 113–126. <https://doi.org/10.1016/j.gsf.2013.03.006>
- Salisbury, M.J., Bohron, W.A., Clyne, M.A., Ramos, F.C., Hoskin, P., 2008. Multiple plagioclase crystal populations identified by crystal size distribution and in situ chemical data: Implications for timescales of magma chamber processes associated with the 1915 eruption of Lassen Peak, CA. *J. Petrol.* 49, 1755–1780. <https://doi.org/10.1093/petrology/egn045>
- Sigurdsson, H., Houghton, B., McNutt, S., Rymer, H., Stix, J., 2015. *The Encyclopedia of Volcanoes, Second Edition*. Academic Press.
- Słaby, E., Götze, J., Wörner, G., Simon, K., Wrzalik, R., Śmigielski, M., 2008. K-feldspar phenocrysts in microgranular magmatic enclaves: A cathodoluminescence and geochemical study of crystal growth as a marker of magma mingling dynamics. *Lithos* 105, 85–97. <https://doi.org/10.1016/j.lithos.2008.02.006>

- Smith, V.C., Blundy, J.D., Arce, J.L., 2009. A temporal record of magma accumulation and evolution beneath Nevado de Toluca, Mexico, preserved in plagioclase phenocrysts. *J. Petrol.* 50, 405–426. <https://doi.org/10.1093/petrology/egp005>
- Stamatelopoulou-Seymour, K., Vlassopoulos, D., Pearce, T.H., Rice, C., 1990. The record of magma chamber processes in plagioclase phenocrysts at Thera Volcano, Aegean Volcanic Arc, Greece. *Contrib. to Mineral. Petrol.* 104, 73–84. <https://doi.org/10.1007/BF00310647>
- Streck, M.J., 2008. Mineral textures and zoning as evidence for open system processes. *Rev. Mineral. Geochemistry* 69, 595–622. <https://doi.org/10.2138/rmg.2008.69.15>
- Troll, V.R., Donaldson, C.H., Emeleus, C.H., 2004. Pre-eruptive magma mixing in ash-flow deposits of the Tertiary Rum Igneous Centre, Scotland. *Contrib. to Mineral. Petrol.* 147, 722–739. <https://doi.org/10.1007/s00410-004-0584-0>
- Vance, J.A., 1965. Zoning in Igneous Plagioclase : Patchy Zoning. *J. Geol.* 73, 636–651.
- Viccaro, M., Giacomoni, P.P., Ferlito, C., Cristofolini, R., 2010. Dynamics of magma supply at Mt. Etna volcano (Southern Italy) as revealed by textural and compositional features of plagioclase phenocrysts. *Lithos* 116, 77–91. <https://doi.org/10.1016/j.lithos.2009.12.012>
- Von Hillebrandt, C., 1989. Estudio Geovulcanologico del Complejo Vulcanico Cuicocha-Cotacachi y sus aplicaciones, Provincia de Imbabura. Escuela Politecnica Nacional.
- Whitney, D.L., Evans, B.W., 2010. Abbreviations for names of rock-forming minerals. *Am. Mineral.* 95, 185–187. <https://doi.org/10.2138/am.2010.3371>
- Winter, J.D., 2014. *Principles of Igneous and Metamorphic Petrology*, Second. ed. Pearson Education Limited.